A META-ANALYTIC APPROACH TO MAPPING CO-OCCURRENT GREY MATTER VOLUME INCREASES AND DECREASES IN PSYCHIATRIC DISORDERS

Lorenzo Mancuso[1,2], Alex Fornito[3,4], Tommaso Costa[1,2], Linda Ficco[1,2], Donato Liloia[1,2], Jordi Manuello[1,2], Sergio Duca[2], Franco Cauda[1,2]

[1] FOCUS Lab, Department of Psychology, University of Turin, Turin, Italy

[2] GCS-fMRI, Koelliker Hospital and Department of Psychology, University of Turin, Turin, Italy

[3] The Turner Institute for Brain and Mental Health, School of Psychological Sciences, Monash University, Victoria, Australia

[4] Monash Biomedical Imaging, Monash University, Victoria, Australia

Abstract

Numerous studies have investigated gray matter (GM) volume changes in diverse patient groups. Reports of disorder-related GM reductions are common in such work, but many studies also report evidence for GM volume increases in patients. It is unclear whether these GM increases and decreases independent or related in some way. Here, we address this question using a novel meta-analytic network mapping approach. We used a coordinate-based meta-analysis of 64 voxel-based morphometry studies of psychiatric disorders to calculate the probability of finding a GM increase or decrease in one region given an observed change in the opposite direction in another region. Estimating this co-occurrence probability for every pair of brain regions allowed us to build a network of concurrent GM changes of opposing polarity. Our analysis revealed that disorder-related GM increases and decreases are not independent; instead, a GM change in one area is often statistically related to a change of opposite polarity in other areas, highlighting distributed yet coordinated changes in GM volume as a function of brain pathology. Most regions showing GM changes linked to an opposite change in a distal area were located in salience, executive-control and default mode networks, as well as the thalamus and basal ganglia. Moreover, pairs of regions showing coupled changes of opposite polarity were more likely to belong to different canonical networks than to the same one. Our results suggest that regional GM alterations in psychiatric disorders are often accompanied by opposing changes in distal regions that belong to distinct functional networks.

Keywords

Compensation, VBM, psychiatric pathology, morphometric alterations, volumetric increase

Introduction

A large body of neuroimaging studies has investigated how diverse diseases are associated with altered brain structure, most commonly quantified through measures of regional grey matter (GM) volume. The vast majority of studies have focused on mapping localized changes using mass univariate approaches such as voxel-based morphometry (Ashburner and Friston, 2000), but analyses of covariations in regional volume changes are also thought to reveal pathological mechanisms and to reflect the distributed and interconnected nature of the brain (Evans, 2013). By far, most work in this area has focused on understanding GM volume reductions in clinical disease. Not only have several meta-analyses of different diseases shown that such reductions are common (Fornito *et al.*, 2009; Bora *et al.*, 2010, 2011, 2012*a*, *b*; Fusar-Poli *et al.*, 2011; Hallahan *et al.*, 2011; Linkersdörfer *et al.*, 2012; Du *et al.*, 2012; Li *et al.*, 2014, 2018; Stoodley, 2014; Cauda *et al.*, 2014; Foster *et al.*, 2015; Lin *et al.*, 2016; Wise *et al.*, 2017; Wu *et al.*, 2018), and other work suggests that anatomically distributed yet coordinated GM reductions are tied to the underlying connectivity between regions (Seeley *et al.*, 2009; Raj *et al.*, 2012; Zhou *et al.*, 2012; Crossley *et al.*, 2014; Iturria-Medina *et al.*, 2014; Zeighami *et al.*, 2015, Cauda *et al.*, 2018*a*; Manuello *et al.*, 2018; Yau *et al.*, 2018; Zheng *et al.*, 2019). In contrast, GM increases are less commonly considered in clinical neuroimaging studies (Cauda *et al.*, 2011, 2017, 2018*b*; Tatu *et al.*, 2018, Cauda *et al.*, 2019*b*; Ding *et al.*, 2019; Lu *et al.*, 2019), potentially because they might be a rarer consequence of disease and because they can be difficult to explain in the context of pathology. Indeed, while a morphometric decrease can be easily interpreted as a sign of neurodegeneration or neurodevelopmental hyperpruning, the interpretation of a disorder-related GM increase is less clear.

Candidate mechanisms for increased GM include modifications to neuronal tissue, such as neurogenesis (Eriksson *et al.*, 1998), synaptogenesis (Sarrazin *et al.*, 2019) or changes in somal size and density, in addition to changes in glia (Rocha *et al.*, 1998) or neurovasculature (Zatorre *et al.*, 2012). There could be diverse causes of such modifications, which may be related to inflammatory processes (Poletti *et al.*, 2019) that might, for instance, induce astrocytic hypertrophy (Li *et al.*, 2019), or to activity-driven volumetric increases similar to those observed during learning (Zatorre *et al.*, 2012). Medications may also an hypertrophic effect (Torres *et al.*, 2013). Otherwise, a GM increase in

patients compared to controls could derive from a pathologic hypopruning that could characterize neurodevelopmental diseases such as schizophrenia (Keshavan *et al.*, 1994*a*). More trivial reasons, such as case-control differences in hydration, head motion, and various other metabolic and physical confounds may also play a role (Weinberger and Radulescu, 2016).

Some authors hypothesised that GM increases could emerge as a compensatory response to localised damage elsewhere. For instance, Janson and colleagues (Janson *et al.*, 1991) observed neuronal hypertrophy in regions connected to a mesencephalic lesion, which they interpreted as a compensation to the injury. Stevens and colleagues (Stevens, 1992) proposed that hippocampal lesions might produce axonal sprouting and synapse proliferation in deafferented regions, and that these changes should have a compensatory function if the rewiring is adaptive. However, they could also lead to a further impairment if the adaptation is suboptimal. In major depression, cortical thickness studies suggest that an early phase of the disease could be characterized by an increased thickness in some regions, in which provisional compensatory mechanisms take place to overcome the deficits induced by the damage in others (Qiu *et al.*, 2014; Li *et al.*, 2019). Indirect evidence for the existence compensatory changes in GM volume comes from a meta-analysis (Cauda *et al.*, 2014) showing that, in people with autism, a GM decrease in one area is associated with an increase of volume and/or DTI-related measures of connectivity in the white matter tracts connecting the affected area. In functional neuroimaging, several studies suggest the presence of compensatory activations during both healthy ageing and in diverse diseases (eg. Dolcos *et al.*, 2002; Tan *et al.*, 2006; Crossley *et al.*, 2016). For instance, after traumatic brain injury, increased functional connectivity of default mode network (DMN), salience network (SN) and executive control network (ECN) has been observed (Hillary *et al.*, 2014). These findings align with the view that the interconnected architecture of the brain means that pathology is seldom defined to a single locus, and may induce distributed responses that are both adaptive and/or maladaptive (Fornito *et al.*, 2015).

If compensatory changes in GM volume do occur in the diseased brain, or if disorder-related GM increases and decreases are more broadly coordinated in some way, then we should expect that these changes should be statistically associated across different disorders. To test this hypothesis, we extended a coordinate-based meta-analytic methodology developed by our group (Cauda *et al.*, 2018*b*; Manuello *et al.*, 2018; Tatu *et al.*, 2018) to calculate the probability of co-occurence between GM increases and decreases in VBM studies of psychiatric disease. This probability quantifies the likelihood that a GM increase or decrease in one brain area co-occurs with a GM change of opposite

polarity in another area. We adopted a transdiagnostic approach, considering all the brain disorders that would show an association between GM decreases and increases, to identify disease-invariant co-alteration mechanisms of brain pathology (Buckholtz and Meyer-Lindenberg, 2012, Cauda *et al.*, 2018*b*). Thus, we aimed to obtain a network of GM co-alterations of opposing polarity (COA-O) that identifies pairs of regions for which there is a statistical dependence between these two opposite forms of GM change. Given prior work indicating that networks of co-alterations (i.e., GM changes of the same polarity) are related to normative connectivity patterns (Yates, 2012, Cauda *et al.*, 2018*b*; Raj and Powell, 2018), we further hypothesised that the COA-O network would show a significant correlation with functional connectivity (FC) networks in healthy individuals.

Material and Methods

Data collection

We adopted the Cochrane Collaboration definition of meta-analysis (Green *et al.*, 2008) and the "PRISMA statement" international guidelines for the selection of studies (Liberati *et al.*, 2009; Moher *et al.*, 2009). Coordinates of statistically significant GM changes were obtained from the BrainMap database (http://brainmap.org/) (Fox and Lancaster, 2002; Fox *et al.*, 2005; Laird *et al.*, 2005; Vanasse *et al.*, 2018).

Two queries were conducted on the VBM BrainMap section (November 2019) to retrieve data on morphometric decreases and increases, respectively:

1) [Experiments Context is Disease] AND [Experiment Contrast is Gray Matter] AND [Experiments Observed Changes is Controls>Patients];

2) [Experiments Context is Disease] AND [Experiment Contrast is Gray Matter] AND [Experiments Observed Changes is Patients>Controls].

We obtained 1001 studies reporting GM decreases and 382 studies reporting GM increases. All the selected experiments with a sample size smaller than 8 participants were eliminated, in line with Scarpazza et al. (2015), who showed that VBM experiments with more than 8 subjects should not be biased by an increased false positive rate. Then we coded the experiments according to the ICD-10

classification (World Health Organisation, 1992), to exclude the non-neurologic and non-psychiatric diseases from the database. In order to quantify the co-occurrence of decreases and increases, we further selected only those couples of experiments (i.e. set of foci resulting by a given statistical comparison) that reported opposing changes between the same groups of patients and healthy controls. Such selection resulted in 170 experiments (85 decreases exp., 85 increases exp.), further reduced to 128 after the exclusion of neurological diseases. See Table 1 and 2 for a list of the experiments and disorders considered.

INSERT TABLE 1 AND 2 HERE

To obtain two control datasets of common change (i.e., datasets in which only GM decreases or only GM increases were reported), we selected from the total pool of 1382 experiments, those considering the 9 conditions we focus on, obtaining 280 experiments for GM decreases and 115 experiments for GM increases (Note: this selection did not require the constraint that increases and decreases be reported in the same study; see Fig. S1 for the PRISMA flow chart and Tables S1 and S2 for the lists of experiments included in the control analyses). We will refer to those two control network of decrease-only and increase-only as COA-D and COA-I, respectively.

Quantifying co-alteration probabilities

Our method is based on the Anatomical Likelihood Estimation (ALE) (Eickhoff *et al.*, 2009, 2012; Turkeltaub *et al.*, 2012). The ALE is a coordinate-based meta-analytic technique that aims to produce a map as the union of a set of modelled alteration (MA) maps, each one representing one statistical comparison (i.e. experiment) included in the study. For each experiment, its MA map is produced creating a 3-D Gaussian distribution of probability around each reported focus of alteration (Eickhoff *et al.*, 2009).Their union produce a (unthresholded) ALE map, which represent the statistical distribution of the alterations across the experiments.

INSERT FIGURE 1 HERE

Our aim is to quantify the degree to which a GM change in one brain region is associated with a change of opposite polarity in another area. We do this for all possible pairs of brain regions, thus building a meta-analytic COA-O network. To build the network we need a unique set of nodes that can represent both the loci of both decreases and increases, and a set of maps that describe the alterations reported by the literature. To obtain the alteration maps from the foci retrieved from the BrainMap database, we computed a MA map for each experiment. To obtain the set of nodes, two unthresholded ALE maps were produced with GingerALE (http://www.brainmap.org/ale/) by merging the GM increase and GM decrease MA maps in the main dataset. When merging, we took the maximum value of the two maps for each voxel (Fig. 1 A). The merged map represents a common spatial distribution of the GM changes in our database. This map was then fed to a peak detection algorithm to identify the coordinates of alteration (Fig. 1 B). The nodes for the COA-D and COA-I were obtained using the same algorithm on the two ALE maps of the two control datasets, producing 233 nodes for the GM-decrease network and 269 nodes for the GM-increase network. Defining network nodes in this data-driven way allows us to more accurately sample the spatial locations of actual GM changes and, critically, to create equally-sized ROIs. In fact, each ROI was considered as altered in a given experiment if the 20% of its voxels were included in the corresponding MA map, thresholded at $p < 0.05$ (Fig 1 C). Since the probability indexes used in the analyses requires binary data of alteration (i.e. a node can be only altered or not, see below), this filtering step was necessary to avoid false positive alterations (i.e. labelling a node as altered if it contains only the periphery of a probability distribution). Although the 20% threshold is arbitrary, it has been previously shown that other thresholds do not change radically the results (Mancuso *et al.*, 2019). Therefore, small ROIs are more likely to reach such threshold of alteration, thus having equally sized nodes would avoid such bias. However, to prove that our results would hold to different methodological choices, we also replicated the network using a pre-defined parcellation based on the Brainnetome Atlas (Fan *et al.*, 2016).

This procedure was repeated on each dataset, resulting in 4 node x experiment matrices of GM changes (i.e., two paired 255x64 matrices of decrease-only and increase only for the main analysis, and two 233x280 and 269x115 matrices for the two decrease-only and increase-only control networks). The

probability of observing a co-occurrent change in each pair of nodes was estimated using Patel's κ (Patel *et al.*, 2006). Table 3 illustrates the possible combinations of two given nodes *a* and *b*, along with their marginal probabilities.

INSERT TABLE 3 HERE

Those marginal probabilities are essential for the Patel's κ, which calculates the probability that the two nodes show co-occurring GM changes relative to the probability that they are altered independently, as

$$\kappa = \frac{(\vartheta_1 - E)}{D(max(\vartheta_1) - E) + (1 - D)\big(E - min\ (\vartheta_1)\big)}$$

where

$$E = (\vartheta_1 + \vartheta_2)(\vartheta_1 + \vartheta_3)$$

$$max(\vartheta_1) = min\ (\vartheta_1 + \vartheta_2, \vartheta_1 + \vartheta_3)$$

$$min(\vartheta_1) = max(0, 2\vartheta_1 + \vartheta_2 + \vartheta_3 - 1)$$

$$D = \begin{cases} \dfrac{\vartheta_1 - E}{2(max(\vartheta_1) - E)} + 0.5, if \vartheta_1 \geq E \\ 0.5 - \dfrac{\vartheta_1 - E}{2\big(E - min(\vartheta_1)\big)}, otherwise \end{cases}$$

The numerator in the fraction is the difference between the likelihood that *a* and *b* are altered together and the expected likelihood *E* that *a* and *b* are co-altered under independence; *E* is the prior information of our Bayesian framework that, in a frequentist paradigm, would be disregarded or treated as not fixed by the data (Patel *et al.*, 2006). The denominator is a weighted normalizing constant to restrict the Patel's κ to the range [–1, 1]. The statistical significance ($p = 0.01$) is evaluated through a Monte Carlo simulation that calculates an estimate of $p(\kappa|z)$ by sampling a Dirichlet distribution and determining

the proportion of the samples in which $\kappa > e$, where e is the threshold of statistical significance. The resulting co-alteration matrix (be it COA-O, COA-I, COA-D) comprises values that are proportional to the statistical relationship between the alterations of the considered brain areas.

Crucially, while the co-alteration control matrix was obtained calculating κ between the $1,2,\ldots N$ nodes within their respective nodes x experiments matrices of alteration ($233x280$ for the decrease condition, resulting in a $233x233$ COA-D matrix, and p<0.05 for the increase condition, resulting in a $269x269$ COA-I matrix), the COA-O matrix was produced calculating the κ between nodes $1,2,\ldots 355$ of the $355x64$ decreases matrix and the $1,2,\ldots 355$ nodes of the $355x64$ increases matrix (Fig. 1 D). It must be stressed that the number of nodes that are effectively connected in the final network is less than the 355 found with the peak detection algorithm, as some nodes have no significant edges after the statistical thresholding .

For each edge with a significant κ of the COA-O network, we also calculated Patel's τ (Patel *et al.*, 2006), which evaluates the asymmetries in conditional probabilities of a given pair of nodes as

$$\tau = \begin{cases} 1 - \dfrac{(\vartheta_1 + \vartheta_3)}{(\vartheta_1 + \vartheta_2)}, if \vartheta_2 \geq \vartheta_3 \\ \dfrac{(\vartheta_1 + \vartheta_2)}{(\vartheta_1 + \vartheta_3)} - 1, otherwise \end{cases}$$

A positive value means that node *a* is ascendant to (i.e., has an influence on) node *b*. In practice, it means that when *a* shows an alteration, *b* usually do not; however, when *b* is altered, *a* tend to be altered as well. Therefore, if one of the two nodes is influencing the other, the direction is more likely to go from *a* to *b* than the other way around. In our implementation (Fig. 1 D), a positive value means a possible influence of a GM decrease on an increase.

Resting state functional connectivity

Functional data were retrieved from the Cambridge dataset of the Functional Connectome Project (Biswal *et al.*, 2010). The sample comprises 198 subjects (75M-123F, 18-30 years old). Each scan consists of 119 time points with TR=3. These data were processed with DPABI 3.1, DPARSFa 4.4 (http://rfmri.org/DPARSF) (Yan *et al.*, 2016). The preprocessing steps were i) slice timing correction;

ii) realignment; iii) regression of motion parameters using the Friston-24 model and of white matter and cerebrospinal fluid signals using *a priori* masks; iv) spatial normalization to standard SPM EPI template; v) smoothing with a 4 mm FWHM kernel; vi) scrubbing as in Power et al. (Power *et al.*, 2012).

Then we extracted the functional signal of the 355 ROIs of the COA-O network to calculate the individual matrix of time series correlations, which were then normalized with the Fisher transformation and averaged into a group FC matrix.

To further investigate the relationship between the COA-O network and normative FC, each node was assigned to a resting state network (RSN) of the Yeo7 parcellation (Yeo *et al.*, 2011), plus the cerebellum and a thalamus/basal ganglia masks (Thal/BG) created on the basis of the Brainnettome Atlas.

Fail-safe and dummy-pairs analyses

We might hypothesize that the dataset of the experiments included in the COA-O analysis could be just a subsample of all the possible evidences about GM changes of opposite polarity, thus biasing our results. To assess their robustness, we implemented a modified version of the Fail-safe technique (Acar *et al.*, 2018). The ratio behind that is that we cannot represent the COA-O network as if we gathered all the possible experiments on the matter, but we still can observe what would happen if our sample was much larger. Therefore, we generated 220 couples of random MAs using the fail-safe R script (https://github.com/NeuroStat/GenerateNull). Such MAs couples were progressively introduced in the database 10 at a time, recalculating the network after each injection. Then, the values of the edges of each new network were correlated with those of the original COA-O network. Since it is possible that any injection step could improve the correlation by mere chance, the method can produce random fluctuations in the correlation values, so the procedure was repeated 30 times. The more the network would hold to the injection of noise, the more it could be assumed that our network is an accurate representation of the COA-O phenomenon, even if our dataset was a subsample of a much larger set of experiments.

To calculate the co-alteration matrix, it was necessary to couple an experiment of decreases to the matching experiment of increases obtained on the same subjects. This forced us to discard all the

papers that do not present the opposing statistical contrast between patients and healthy controls group. In general, this meant that we discarded many studies that only reported GM decreases in patients and provided no information about GM increases. There are two possible explanations as to why a study might only report GM decreases. One is that the researchers never tested for GM increases, despite the fact that they actually exist in the patient group. In this case, the data are incomplete and so it is necessary to discard these studies. The second reason is that the researchers ran the contrast, found no evidence of GM increases, and then declined to report the results. In this case, the data are informative and should be included in the analysis. However, there is no way to disambiguate case 1 from case 2, so all non-matched experiments had to be excluded. To evaluate how much this decision impacted on the results, we progressively injected the database with decrease experiments randomly sampled from the control dataset (see Data collection). Each one of these experiments was matched with a dummy increase experiment with no foci. We added 10 of these dummy pairs of experiments to the main database at each time, until we injected 220 dummy pairs, and repeated this procedure 30 times. The same analysis was made with increases. If the results hold to a consistent injection of dummy-pairs in the database, we could conclude that our network do not suffered the decision to exclude the unmatched experiments.

Results

Our first selection of studies produced 85 decrease and 85 increase experiments coupled to each other. Table 1 contains the number of experiments for each of the disorders of such dataset. The distribution of psychiatric and neurological pathologies in those experiments was asymmetrical, with 64 experiments related to 9 psychiatric diagnoses and 21 experiments to 4 neurological ones. Of the latter, 13 were related to epilepsy, the remaining to extrapyramidal and movement disorders ($n = 4$), Parkinson's disease ($n = 2$) and dystonia ($n = 2$). Thus, it seems that the coupling of decreases and increases is more characteristic of psychiatric conditions than neurological ones (with the only exception of the epilepsy), therefore, we decided to focus our analysis only on psychiatric disorders. The COA-O network comprising neurological disorders can be seen at Supplementary Fig. S2.

Decrease-increase association network

The COA-O network for psychiatric diseases is presented in Figure 2. Although our network-mapping procedure produced 355 nodes, only 97 of them (32%) showed statistically significant co-occurrent changes with another region. For this subset of 97 nodes, we identified 292 significant co-occurrence probabilities, which represent edges in the COA-O network. Each edge in this network connects two areas showing GM changes in opposing directions. Of the 97 nodes in the network, 46 showed a GM decrease, 38 showed a GM increase, and 13 showed both (a node can assume both the roles of decrease and increase in different edges)..

GM increases and decreases are not uniformly distributed throughout the network. For instance, the superior parietal lobule (SPL) has a high concentration of areas with increased GM (0 nodes showing a decrease and 6 showing an increase), while the left insula and left inferior frontal gyrus (IFG) contain many nodes of decreased GM (10 decresase nodes, 1 increase node, 3 nodes are both decrease and increase), as showed by their nodal strength. The strengths (i.e. weighted degree centrality) of decreases and increases were calculated as the sum of each row and each column of the COA-O matrix, respectively. Node strength is unevenly distributed between hemispheres, with the left hemisphere having higher strength nodes than the right (Fig. 2 B). In fact, of the 25 nodes with highest strength, only 5 were in the right hemisphere (Table 4). Involvement of regions in the occipital lobe and posterior temporal lobes, and anterior prefrontal cortex, in the network is sparse. Most of the nodes, especially the ones with high strength, are situated in the anterior temporal and inferior frontal cortices, thalamus, and basal ganglia.

These findings were replicated using the Brainnetome atlas, producing a similar network and thus demonstrating that our method is independent of the node definition procedure (Fig. S4).

INSERT FIGURE 2 AND TABLE 4 HERE

Relationship between co-occurrent changes and functional connectivity

Contrary to our first hypothesis, the 292 significant Patel's κ values of the COA-O matrix were not correlated with the 292 corresponding Pearson's r values of the FC matrix ($r = -0.07$, non-significant at p=0.05). If COA-O edges were correlated to FC, it could be expected that most of them connected nodes belonging to a same canonical resting state networks (RSN), within which FC values tend to be

high. Given the lack of correlation between our COA-O edges and normative FC, we hypothesised that the edges of the COA-O network tend to connect nodes belonging to different RSNs. Thus, each node was assigned to one of the RSN of the Yeo7 parcellation (Yeo *et al.*, 2011), plus the cerebellum and the Thal/BG. Of the 292 edges, only 49 are between nodes of the same RSN, whereas 83% link nodes that belong to different RSNs. In comparison, COA-I and COA-D networks have a lower fraction of between-RSNs edges. The between-RSN edges of the COA-D network represent 78% of the total; the fraction is 68% for the COA-I. To evaluate the statistical significance of these differences, we randomized the COA-O, COA-D and COA-I networks using the Maslov-Sneppen algorithm (Maslov and Sneppen, 2002; Rubinov and Sporns, 2010) to preserve the degree distribution of each network. We then computed the differences in between-RSN edge fractions between the randomized networks and repeated the process 1000 times to build an empirical null distribution. The observed between-RSN fractions were significantly higher for the difference between the COA-O network and COA-D network ($p<0.001$) and between the COA-O network and COA-I network ($p<0.001$). Thus, although in comparison with with the COA-D network the difference is only of 5% (13% with the COA-I network), co-occurrent GM changes of opposing polarity are significantly more likely the occur between brain regions belonging to different functional networks.

(Maslov and Sneppen, 2002; Rubinov and Sporns, 2010)Focusing on the COA-O network, many between RSN edges are incident upon DMN nodes (Fig. 3). Most nodes mapped to the DMN show decreased GM, thus the areas to which these nodes connect in the COA-O network almost always show increased GM (especially Thal/BG, salience andexecutive control networks). The DMN is also the RSN with more nodes in the COA-D network, but it is poorly represented in the COA-I network, further supporting a higher frequency of GM reductions in this brain network. Almost all COA-O edges within the DMN connect to a single node showing increased GM located in the ventromedial prefrontal cortex ({x,y,z} = [-16, 34, -4]). This indicates that is is relatively rare to find co-occurring GM increases and decreases within the DMN.

As with the DMN, the ECN and, overall, the SN mostly comprise nodes showing GM decreases. In contrast, the dorsal attention network (DAN) is comprised almost only of nodes showing GM increases, located in the SPL (Fig. 2), and mostly associated with decreases in the Thal/BG and IFG (Fig. 2, Fig. 3 and Table S3). The cerebellum has only two increase nodes associated to the DMN and the ECN and that were not replicated using the Brainnetome atlas. In general, most edges of the COA-O are focused

on regions in the telencephalon. A table listing all edges can be found in the Supplementary Materials (Table S3).

INSERT FIGURE 3 HERE

The node distribution across RSN is non-random. The DMN and Thal/BG are the RSNs with more nodes, while the cerebellum and visual network are the less represented. To evaluate if this spatial distribution is statistically significant, we randomly picked 97 nodes from a homogeneous parcellation (Fornito *et al.*, 2010; Zalesky *et al.*, 2010). A permutation test showed that, apart from the DMN, all the RSNs have a number of nodes significantly different from the null model ($p = 0.05$, one-tailed t-test, 10000 permutations). RSNs with few nodes have less nodes than expected from chance (Visual, $p < 0.001$; Sensorimotor, $p = 0.0398$; DAN, $p = 0.0119$; Cerebellum, $p < 0.001$), while the bigger ones have significantly more nodes (Salience, $p = 0.0105$; Limbic, $p = 0.0326$, Executive control, $p = 0.0381$; Thal/bg, $p < 0.001$).

Fail-safe and dummy-pairs analyses

As our COA-O dataset of experiments is relatively small, we assessed the robustness of our results to the injection of noise with a modified Fail-safe technique (Acar *et al.*, 2018). We observed that the COA-O network is still correlated with $r \approx 0.3$ even after we added 220 null maps (~350% of the original dataset, Fig. 3 C). This means that, if our dataset was much larger, the network might remain relatively stable, unless the injection of real data was somehow much more harmful to the results than that of null studies.

To verify that our results were not severely affected by the necessity of including only the couple of experiments showing opposing GM changes, we added a set of uncoupled experiments, paired with an empty one. The results can be seen at Fig. 3 D and E. The network resulting from the addition of 220 decrease experiments paired with empty ones correlates with the original one at r=0.88 (averaged across 30 runs). Applying the same procedure adding only GM increase experiments produced a network that correlated with the original one, on average, r=0.79. Thus, our results would if we did not exclude non-matching experiments.

Directionality of the decrease-increase associations

We further assessed the directionality of the edges of the COA-O network using the Patel's τ, which compares the conditional probabilities of having an alteration of region A given a change in B and of a change in B given a change in A. A positive edge means that it is more probable to have an increase given a decrease than the other way round, while a negative edge means that it is more probable to have an increase given a decrease. The τ network is characterized by both positive and negative edges (Fig. 4) although positive edges are slightly stronger and more numerous. Many negative edges are incident upon nodes of the parietal lobe that are characterized by GM increases. Conversely, the nodes in the left IFG and the thalamus, which represent areas of GM decrease, are connected by many positive edges (Fig 4 and S5). Many positive edges link a decrease of the salience network or the DMN to a decrease in the Thal/BG, but also DMN to SN and SN to limbic network. Negative edges are more distributed across RSNs (Fig. 4). In general. these findings indicate that the edges of the COA-O network are often directed from the decrease nodes to the increase nodes, but also the opposite can be true.

INSERT IMAGE 4 HERE

Discussion

Our meta-analytic network mapping procedure evaluated the statistical relationship between GM increases and decreases across neurological and psychiatric disorders. Co-occurrent decreases and increases in GM volume are rarely reported in neurological diseases, with epilepsy being an exception. Conversely, such co-occurrent changes where more common in psychiatric disorders. This result might reflect a reporting bias in the neurology literature to focus only on GM decreases,However, it may also represent a genuine increase in the likelihood of observing GM increases in psychiatric disorders and epilepsy. In fact, a common thread linking these two is that many of them have a neurodevelopmental origin, which may provide greater opportunity for plastic adaptations and thus the emergence of GM increases.

In psychiatric disorders, our analysis revealed that GM increases and decreases are not independent; instead, many areas show a GM change that is statistically related to a change of opposite polarity in

other areas. The resulting COA-O network presents a series of interesting features. For instance, there appears to be a preponderance of left hemisphere nodes being more strongly involved in such coordinated GM changes (Fig. 2). The left hemisphere dominance in the COA-O network is intriguing and might suggest a differential involvement of the two hemispheres in the anatomy of psychiatric disorders. This observation is reminiscent of the recent finding that the hubs of the COA-D are symmetric across the hemispheres to those of the COA-I network (Cauda *et al.*, 2019*a*), in the fact that they both highlight how the two hemispheres might be differently involved by opposing GM alterations.

The nodes involved in the COA-O phenomenon are not randomly distributed across the networks. In particular, the SN and ECN showed more nodes than expected by chance, consistent with their presumed importance in psychiatric pathology (Palaniyappan and Liddle, 2012; Goodkind *et al.*, 2015; McTeague *et al.*, 2016, 2017; Sheffield *et al.*, 2017; Sha *et al.*, 2019). The thalamus and basal ganglia also showed more significant nodes than expected by whereas the DMN does not. In fact, most canonical RSNs contained significantly fewer COA-O nodes than expected by chance. Notably, while the Thal/BG showed an approximately equal number of decrease and increase nodes, the DMN is mostly characterized by decreases. Such decreases were often found to be associated to Thal/BG increases, and increases in the the SN and ECN. The ECN and, to a lesser extent, the SN, show a similar propensity for decrease nodes associated with Thal/BG increases, indicating that GM decreases in the three higher order cortical networks are often accompanied by GM increases in subcortical structures.

Another relevant aspect of the COA-O network was the tendency of its edges to connect different RSNs. In fact, analysing the COA-O network for psychiatric disorders, we observed that it is not correlated to FC, and that its edges tend to connect different RSNs. Prior work has shown a closer association between FC and co-occurrent GM decreases or increases, which can be largely explained by models of diffusion along connectivity pathways (Cauda *et al.*, 2018*b*; Raj and Powell, 2018). Our findings thus suggest that co-occurent GM changes of opposing polarity may emerge through a distinct phenomenon. Candidate mechanisms include effects of medication, direct effects of disease, or compensatory or maladaptive responses to insult.

GM increases due to medication

It is possible that increased GM in psychiatric disorders is not due to the disease process, but instead reflects a secondary consequence of medication. For instance, it has been reported that lithium, commonly used to treat bipolar disorder, has a neurotrophic and morphometric increase effect (Manji *et al.*, 1997, 1999; Moore *et al.*, 2000; Chen *et al.*, 2000; Fukumoto *et al.*, 2001; Sassi *et al.*, 2002; Angelucci *et al.*, 2003; Hashimoto *et al.*, 2003; Beyer *et al.*, 2004; Frey *et al.*, 2006; Bearden *et al.*, 2007; Monkul *et al.*, 2007; Yucel *et al.*, 2007; Bearden *et al.*, 2008; Yucel *et al.*, 2008; Kempton *et al.*, 2008; Hammonds and Shim, 2009; Lyoo *et al.*, 2010; Hajek *et al.*, 2012; López-Jaramillo *et al.*, 2017; Hibar *et al.*, 2018). Similarly, the use of conventional antipsychotics has repeatedly been associated with basal ganglia (Muller and Seeman, 1977; Chakos *et al.*, 1994, 1998, Keshavan *et al.*, 1994*b*; Murali *et al.*, 1995; Sedvall *et al.*, 1995; Shihabuddin *et al.*, 1998; Kippin *et al.*, 2005; Chopra *et al.*, 2020)(Kippin *et al.*, 2005) and thalamic (Gur *et al.*, 1998; Strungas *et al.*, 2003; Dazzan *et al.*, 2005) anatomic increases.

Given that many patients included in our meta-analysis were undergoing medication at the time of the scan (Table S4), this variable is likely to have some impact on the COA-O network. However, there is some evidence that suggests that medication alone is unable to explain our results: first, morphological effects of medication are often found to be localized to restricted regions, such as medial temporal lobe and subgenual cortex with lithium (Germaná *et al.*, 2010; Hafeman *et al.*, 2012) and BG with antypsichotics (Navari and Dazzan, 2009), while our increase nodes are situated in many other brain areas; second, some studies report that medications could attenuate pathological decreases rather than increase GM volume in patients compared to controls (Sheline *et al.*, 2003; Wada *et al.*, 2005; Hibar *et al.*, 2016; Zung *et al.*, 2016; Sarrazin *et al.*, 2019); third, atypical antipsychotics, although found by some to be neurotrophic and induce neurogenesis (Wakade *et al.*, 2002; Bai *et al.*, 2003; Halim *et al.*, 2004; Wang *et al.*, 2004; Park *et al.*, 2006) produced mixed volumetric findings (Massana *et al.*, 2005; Navari and Dazzan, 2009) but often no increase effects were found in the BG (Chakos *et al.*, 1995; Frazier *et al.*, 1996; Westmoreland Corson *et al.*, 1999; Lang *et al.*, 2001, 2004; Scheepers *et al.*, 2001). Moreover, a study reports an absence of increased volume of BG also for typical antipsychotics (Kreczmanski *et al.*, 2007); fourth, anticonvulsant drugs, used in the treatment of bipolar disorder but also for epilepsy (the only neurologic disease with a non-negligible number of experiments in our database) showed to produce decreases or no effect (Chang *et al.*, 2009; Germaná *et al.*, 2010; Abé *et al.*, 2016; Hibar *et al.*, 2018); fifth, the increased striatal volume of relatives of schizophrenic patients suggests a genetic factor (Oertel-Knöchel *et al.*, 2012). Similarly, increased cortical thickness and subcortical volume were found also in drug-naive patients with depression (Qiu *et al.*, 2014; Reynolds

et al., 2014; Yang *et al.*, 2015; Zuo *et al.*, 2018; Li *et al.*, 2019; Suh *et al.*, 2019); sixth, patients with autism or development disorders included in our study were not under drug treatment (Table S4). Therefore, it seems that medications alone are unable to explain the phenomenon of DIA; seventh, if GM increases were purely explained by medication, they would most likely be statistically associated to all, or most of, the GM decreases. On the contrary, the nodes of increase were selectively co-altered with one or few decreases. The effect of medication thus cannot provide the sole explanation for the observed findings in the COA-O network.

Co-occurrent increases and decreases as a direct effect of the pathology

One possible hypothesis might be that GM increases are as direct effect of the disease process. Co-occurring GM decreases and increases could arise due to regionally distinct effects of inflammatory processes (Li *et al.*, 2019), or, possibly, altered developmental pruning (Keshavan *et al.*, 1994*a*). Another option could be that, due to dysregulation of ascending neuromodulatory projection systems (Davis *et al.*, 1991; Sesack and Carr, 2002), different areas of the brain may become hyperactivated or hypoactivated, potentially resulting in coordinated and concomitant increases and decreases in volume through activity-dependent plasticity. These changes could be driven by neurodevelopmental miswiring of connectivity, resulting in a de-differentiation of function (Fornito *et al.*, 2015).

Co-occurrent increases and decreases as a form of compensation

Another hypothesis might be that GM increases reflect a compensatory response to decreases. In fact, it has been reported that the brain topology of chronic patients shows modifications that appears to counter or normalize those occurred as consequence of a pathologic perturbation (Lord *et al.*, 2012; Hillary *et al.*, 2015). The seemingly most logical consequence of this view should be that the COA-O would happen between regions with similar function and thus belonging to the same RSN. Indeed, it was previously shown that, in schizophrenic patients, over- and under-activations are often located in topologically close areas (Crossley *et al.*, 2016). Our data are not consistent with this scenario, as COA-O edges are not correlated with FC and are more often between- than within-RSN (Fig. 2). Given prior reports that strongly connected areas tend to share GM changes in the same direction (Cauda *et al.*, 2018*b*; Shafiei *et al.*, 2019), our findings suggest that such regions may have a limited capacity for

compensation, possibly due to diaschisis and other maladaptive responses (Carrera and Tononi, 2014; Fornito *et al.*, 2015). Therefore, a region which is not strongly connected to a damaged area but has a related function may be the best candidate to take on a compensatory role. For instance, the SPL nodes of increases are especially associated with decreases in the insula/IFG and Thal/BG. Despite belonging to distinct RSNs, these areas have all been implicated in pain perception (Chudler and Dong, 1995; Strigo *et al.*, 2003; Fitzek *et al.*, 2004; Lu *et al.*, 2004; Kong *et al.*, 2006; Schoedel *et al.*, 2008; Freund *et al.*, 2009; Tseng *et al.*, 2010; Bräscher *et al.*, 2016), somatosensory perception in general (Olausson *et al.*, 2002, 2005; Yoo *et al.*, 2003; Stoeckel *et al.*, 2004; Nagy *et al.*, 2006; Robbe, 2018), and motor functions (Stephan *et al.*, 1995; Kertzman *et al.*, 1997; Binkofski *et al.*, 1999; Jovicich *et al.*, 2001; Herrero *et al.*, 2002; Groenewegen, 2003; Lotze *et al.*, 2006; Beurze *et al.*, 2007; Naito *et al.*, 2008; Langner *et al.*, 2014), although the SPL can also be associated to top-down attention as part of the DAN (Corbetta and Shulman, 2002; Yeo *et al.*, 2011).

The concept of compensation usually involves an adaptive change for the individual, however some have suggested that neuroplastic modifications consequential to psychiatric diseases might also be dysfunctional for the patient well-being (Amad *et al.*, 2019; Palaniyappan, 2019).

Directionality of the associations

Using Patel's τ, we also produced a directed network of COA-O, representing the ascendancy (influence) of decreases to increases. The resulting network shows a clear separation of positive and negative edges, with the former being more prevalent between fronto-temporal nodes and the latter being incident upon parietal nodes (Fig. 4). Although this is an interesting observation that suggests that the COA-O mechanisms might work differently in distinct parts of the brain, there are several possible explanations for this observation. Critically, while the unbalance of conditional probabilities might indicate an influence of a node on the other, it could result also from the action of a third agent. In fact, if node *a* and *b* are both influenced by an element external to the couple, but one of the two nodes is more vulnerable to its action than the other, we would obtain the same unbalanced probabilities of alteration. Such a third agent could be another node or the pathology itself, to which the two regions would be differently vulnerable. Such differential vulnerability expresses in two ways: one of the nodes undergo a GM decrease while the other an increase, and one of the two node is more likely to be modified than the other. Therefore, the ascendancy as we calculated it could be either interpreted

as a measure of influence of a node on the other, or as an evidence of a sort of primacy of a node over the other in the system of COA-O. In fact, considering that the COA-O edges do not correspond to those of FC, the hypothesis of a direct influence of a node on another seems the less likely of the two.

Limitations and future directions

The main limitation of this study comes from a relatively small sample of included experiments. Although we adopted a transdiagnostic approach, only 64 comparisons reported both increases and decreases on psychiatric patients in the BrainMap database. We suspect increases can be sometimes overlooked and not reported by some authors, producing a file-drawer effect. However, our Fail-safe technique showed that our network remains relatively preserved also after the injection of ~350% of noise, reassuring us about the validity of our results. Moreover, even if we include non-coupled experiments, the network remains remarkably similar, indicating that the COA-O edges can be attenuated, but not radically changed if including papers that do not presented both GM changes in the database.

The transdiagnostic approach embraced here was motivated by the interest in general brain mechanisms of COA-O, but disease-specific investigations would be of great interest as well. The scarcity of experiments retrieved by our search prevented us to do so, but future meta-analyses might be able to gather more data.

Longitudinal or cross-sectional studies are also needed to ascertain the presence of COA-O in individual's brains Moreover, functional neuroimaging and clinical assessment would be critical to evaluate the eventual compensatory function of the COA-O phenomenon.

The use of the Patel's τ has been advocated by some as a valid method to investigate network directionality (Smith *et al.*, 2011), but its use in effective connectivity has also been severely questioned by others (Wang *et al.*, 2017). However, our study did not used the Patel's τ in search of a strict causal directionality, but to investigate a more general notion of directionality between nodes.

Conclusions

Our analysis provides evidence for coordinated GM decreases and increases in psychiatric disorders, with such coordinated changes principally affecting higher-order association networks and subcortical regions. Our findings (Adachi *et al.*, 2012)open a new line of research into the mechanisms underlying coordinated GM changes of opposing polarity, and we hope that they draw greater attention on the often-neglected GM increases observed in patients.

Funding

This study was supported by Fondazione Sanpaolo, Turin (Cauda F. PI).

Competing interested

The authors declare no competing interest.

Abé C, Ekman CJ, Sellgren C, Petrovic P, Ingvar M, Landén M. Cortical thickness, volume and surface area in patients with bipolar disorder types I and II. J Psychiatry Neurosci 2016; 41: 240–250.

Acar F, Seurinck R, Eickhoff SB, Moerkerke B. Assessing robustness against potential publication bias in Activation Likelihood Estimation (ALE) meta-analyses for fMRI. PLoS One 2018; 13: 1–23.

Adachi Y, Osada T, Sporns O, Watanabe T, Matsui T, Miyamoto K, et al. Functional connectivity between anatomically unconnected areas is shaped by collective network-level effects in the macaque cortex. Cereb Cortex 2012; 22: 1586–1592.

Amad A, Expert P, Lord L-D, Fovet T, Geoffroy PA. Plastic Adaptation to Pathology in Psychiatry: Are Patients with Psychiatric Disorders Pathological Experts? Neurosci 2019: 107385841986708.

Angelucci F, Aloe L, Jiménez-Vasquez P, Mathé AA. Lithium treatment alters brain concentrations of nerve growth factor, brain-derived neurotrophic factor and glial cell line-derived neurotrophic factor in a rat model of depression. Int J Neuropsychopharmacol 2003; 6: 225–231.

Ashburner J, Friston KJ. Voxel-based morphometry - The methods. Neuroimage 2000; 11: 805–821.

Bai O, Chlan-Fourney J, Bowen R, Keegan D, Li XM. Expression of brain-derived neurotrophic factor mRNA in rat hippocampus after treatment with antipsychotic drugs. J Neurosci Res 2003; 71: 127–131.

Bearden CE, Thompson PM, Dalwani M, Hayashi KM, Lee AD, Nicoletti M, et al. Greater Cortical Gray Matter Density in Lithium-Treated Patients with Bipolar Disorder. Biol Psychiatry 2007; 62: 7–16.

Bearden CE, Thompson PM, Dutton RA, Frey BN, Peluso MAM, Nicoletti M, et al. Three-dimensional mapping of hippocampal anatomy in unmedicated and lithium-treated patients with bipolar disorder. Neuropsychopharmacology 2008; 33: 1229–1238.

Beurze SM, De Lange FP, Toni I, Medendorp WP. Integration of target and effector information in the human brain during reach planning. J Neurophysiol 2007

Beyer JL, Kuchibhatla M, Payne ME, Moo-Young M, Cassidy F, MacFall J, et al. Hippocampal volume measurement in older adults with bipolar disorder. Am J Geriatr Psychiatry 2004; 12: 613–620.

Binkofski F, Buccino G, Stephan KM, Rizzolatti G, Seitz RJ, Freund HJ. A parieto-premotor network for object manipulation: Evidence from neuroimaging. In: Experimental Brain Research. 1999

Biswal BB, Mennes M, Zuo X-N, Gohel S, Kelly C, Smith SM, et al. Toward discovery science of human brain function. Proc Natl Acad Sci 2010; 107: 4734–4739.

Bora E, Fornito A, Pantelis C, Yücel M. Gray matter abnormalities in Major Depressive Disorder: A meta-analysis of voxel based morphometry studies. J Affect Disord 2012; 138: 9–18.

Bora E, Fornito A, Radua J, Walterfang M, Seal M, Wood SJ, et al. Neuroanatomical abnormalities in schizophrenia: A multimodal voxelwise meta-analysis and meta-regression analysis. Schizophr Res 2011; 127: 46–57.

Bora E, Fornito A, Yücel M, Pantelis C. Voxelwise Meta-Analysis of Gray Matter Abnormalities in Bipolar Disorder. Biol Psychiatry 2010; 67: 1097–1105.

Bora E, Fornito A, Yücel M, Pantelis C. The effects of gender on grey matter abnormalities in major psychoses: A comparative voxelwise meta-analysis of schizophrenia and bipolar disorder. Psychol Med 2012; 42: 295–307.

Bräscher AK, Becker S, Hoeppli ME, Schweinhardt P. Different brain circuitries mediating controllable and uncontrollable pain. J Neurosci 2016

Buckholtz JW, Meyer-Lindenberg A. Psychopathology and the Human Connectome: Toward a Transdiagnostic Model of Risk For Mental Illness. Neuron 2012; 74: 990–1004.

Carrera E, Tononi G. Diaschisis: Past, present, future. Brain 2014; 137: 2408–2422.

Cauda F, Costa T, Nani A, Fava L, Palermo S, Bianco F, et al. Are schizophrenia, autistic, and obsessive spectrum disorders dissociable on the basis of neuroimaging morphological findings?: A voxel-based meta-analysis. Autism Res 2017; 10: 1079–1095.

Cauda F, Costa T, Palermo S, D'Agata F, Diano M, Bianco F, et al. Concordance of white matter and gray matter abnormalities in autism spectrum disorders: A voxel-based meta-analysis study. Hum Brain Mapp 2014; 35: 2073–2098.

Cauda F, Geda E, Sacco K, D'Agata F, Duca S, Geminiani G, et al. Grey matter abnormality in autism spectrum disorder: An activation likelihood estimation meta-analysis study. J Neurol Neurosurg Psychiatry 2011; 82: 1304–1313.

Cauda F, Mancuso L, Nani A, Manuello J, Liloia D, Gelmini G, et al. Hubs of long-distance co-alteration in brain pathology [Internet]. bioRxiv 2019Available from: https://www.biorxiv.org/content/10.1101/846642v1

Cauda F, Nani A, Costa T, Palermo S, Tatu K, Manuello J, et al. The morphometric co-atrophy networking of schizophrenia, autistic and obsessive spectrum disorders. Hum Brain Mapp 2018; 39:

1898–1928.

Cauda F, Nani A, Manuello J, Liloia D, Tatu K, Vercelli U, et al. The alteration landscape of the cerebral cortex. Neuroimage 2019; 184: 359–371.

Cauda F, Nani A, Manuello J, Premi E, Palermo S, Tatu K, et al. Brain structural alterations are distributed following functional, anatomic and genetic connectivity. Brain 2018; 141: 3211–3232.

Chakos MH, Lieberman JA, Alvir J, Bilder R, Ashtari M. Caudate nuclei volumes in schizophrenic patients treated with typical antipsychotics or clozapine. Lancet 1995; 345: 456–457.

Chakos MH, Lieberman JA, Bilder RM, Borenstein M, Lerner G, Bogerts B, et al. Increase in caudate nuclei volumes of first-episode schizophrenic patients taking antipsychotic drugs. Am J Psychiatry 1994; 151: 1430–1436.

Chakos MH, Shirakawa O, Lieberman J, Lee H, Bilder R, Tamminga CA. Striatal enlargement in rats chronically treated with neuroleptic. Biol Psychiatry 1998; 44: 675–684.

Chang K, Karchemskiy A, Kelley R, Howe M, Garrett A, Adleman N, et al. Effect of divalproex on brain morphometry, chemistry, and function in youth at high-risk for bipolar disorder: A pilot study. J Child Adolesc Psychopharmacol 2009; 19: 51–59.

Chen G, Rajkowska G, Du F, Seraji-Bozorgzad N, Manji HK. Enhancement of hippocampal neurogenesis by lithium. J Neurochem 2000; 75: 1729–1734.

Chopra S, Fornito A, Francey S, O'Donoghue B, Cropley V, Nelson B, et al. Differentiating the Effect of Medication and Illness on Brain Volume Reductions in First-Episode Psychosis: A Longitudinal, Randomized, Triple-blind, Placebo-controlled MRI study. medRxiv 2020; 13: 2020.03.18.20038471.

Chudler EH, Dong WK. The role of the basal ganglia in nociception and pain. Pain 1995

Corbetta M, Shulman GL. Control of goal-directed and stimulus-driven attention in the brain. Nat Rev Neurosci 2002; 3: 201–215.

Crossley NA, Mechelli A, Ginestet C, Rubinov M, Bullmore ET, McGuire P. Altered Hub Functioning and Compensatory Activations in the Connectome: A Meta-Analysis of Functional Neuroimaging Studies in Schizophrenia. Schizophr Bull 2016; 42: 434–442.

Crossley NA, Mechelli A, Scott J, Carletti F, Fox PT, Mcguire P, et al. The hubs of the human connectome are generally implicated in the anatomy of brain disorders. Brain 2014; 137: 2382–2395.

Davis KL, Kahn RS, Ko G, Davidson M. Dopamine in schizophrenia: A review and reconceptualization. Am J Psychiatry 1991; 148: 1474–1486.

Dazzan P, Morgan KD, Orr K, Hutchinson G, Chitnis X, Suckling J, et al. Different effect of typical and atypical antipsychotics on grey matter in first episode psychosis: The ÆSOP study. Neuropsychopharmacology 2005; 30: 765–774.

Ding Y, Ou Y, Pan P, Shan X, Chen J, Liu F, et al. Brain structural abnormalities as potential markers for detecting individuals with ultra-high risk for psychosis: A systematic review and meta-analysis. Schizophr Res 2019; 209: 22–31.

Dolcos F, Rice HJ, Cabeza R. Hemispheric asymmetry and aging□: Right hemisphere decline or asymmetry reduction Hemispheric asymmetry and aging□: right hemisphere decline or asymmetry reduction. Neurosci Biobehav Rev 2002; 7634: 819–825.

Du MY, Wu QZ, Yue Q, Li J, Liao Y, Kuang WH, et al. Voxelwise meta-analysis of gray matter reduction in major depressive disorder. Prog Neuro-Psychopharmacology Biol Psychiatry 2012; 36: 11–16.

Eickhoff S, Laird A, Grefkes C, Wang LE, Zilles K, Fox PT. Coordinate-based ALE meta-analysis of neuroimaging data: a random-effects approach based on empirical estimates of spatial uncertainty. Hum Brain Mapp 2009; 30: 2907–2926.

Eickhoff SB, Bzdok D, Laird AR, Kurth F, Fox PT. Activation likelihood estimation revisited. Neuroimage 2012; 59: 2349–2361.

Eriksson PS, Perfilieva E, Björk-Eriksson T, Alborn AM, Nordborg C, Peterson DA, et al. Neurogenesis in the adult human hippocampus. Nat Med 1998; 4: 1313–1317.

Evans AC. Networks of anatomical covariance. Neuroimage 2013; 80: 489–504.

Fan L, Li H, Zhuo J, Zhang Y, Wang J, Chen L, et al. The Human Brainnetome Atlas: A New Brain Atlas Based on Connectional Architecture. Cereb Cortex 2016; 26: 3508–3526.

Fitzek S, Fitzek C, Huonker R, Reichenbach JR, Mentzel HJ, Witte OW, et al. Event-related fMRI with painful electrical stimulation of the trigeminal nerve. Magn Reson Imaging 2004

Fornito A, Yücel M, Patti J, Wood SJ, Pantelis C. Mapping grey matter reductions in schizophrenia: An anatomical likelihood estimation analysis of voxel-based morphometry studies. Schizophr Res 2009; 108: 104–113.

Fornito A, Zalesky A, Breakspear M. The connectomics of brain disorders. Nat Rev Neurosci 2015; 16: 159–172.

Fornito A, Zalesky A, Bullmore ET. Network scaling effects in graph analytic studies of human resting-state fMRI data. Front Syst Neurosci 2010; 4: 1–16.

Foster NEV, Doyle-Thomas KAR, Tryfon A, Ouimet T, Anagnostou E, Evans AC, et al. Structural Gray Matter Differences during Childhood Development in Autism Spectrum Disorder: A Multimetric Approach. Pediatr Neurol 2015; 53: 350–359.

Fox PT, Laird AR, Fox SP, Fox PM, Uecker AM, Crank M, et al. BrainMap taxonomy of experimental design: Description and evaluation. Hum Brain Mapp 2005; 25: 185–198.

Fox PT, Lancaster JL. Mapping context and content: The BrainMap model. Nat Rev Neurosci 2002; 3: 319–321.

Frazier A, Giedd JN, Rapoport JL. Childhood-onset schizophrenia: brain MRI rescan after 2 years of clozapine maintenance treatment. Am J Psychiatry 1996; 153: 564–566.

Freund W, Klug R, Weber F, Stuber G, Schmitz B, Wunderlich AP. Perception and suppression of thermally induced pain: A fMRI study. Somatosens Mot Res 2009

Frey BN, Andreazza AC, Ceresér KMM, Martins MR, Valvassori SS, Réus GZ, et al. Effects of mood stabilizers on hippocampus BDNF levels in an animal model of mania. Life Sci 2006; 79: 281–286.

Fukumoto T, Morinobu S, Okamoto Y, Kagaya A, Yamawaki S. Chronic lithium treatment increases the expression of brain-derived neurotrophic factor in the rat brain. Psychopharmacology (Berl) 2001; 158: 100–106.

Fusar-Poli P, Borgwardt S, Crescini A, Deste G, Kempton MJ, Lawrie S, et al. Neuroanatomy of vulnerability to psychosis: A voxel-based meta-analysis. Neurosci Biobehav Rev 2011; 35: 1175–1185.

Germaná C, Kempton MJ, Sarnicola A, Christodoulou T, Haldane M, Hadjulis M, et al. The effects of lithium and anticonvulsants on brain structure in bipolar disorder. Acta Psychiatr Scand 2010; 122: 481–487.

Goodkind M, Eickhoff SB, Oathes DJ, Jiang Y, Chang A, Jones-Hagata LB, et al. Identification of a common neurobiological substrate for mental illness. JAMA psychiatry 2015; 72: 305–15.

Green S, Higgins JP, Alderson P, Clarke M, Mulrow CD, Oxman AD. Introduction. In: Higgins JP, Green S, editor(s). Cochrane Handbook for Systematic Reviews of Interventions. Chichester, UK: John

Wiley & Sons, Ltd; 2008. p. 1–9

Groenewegen HJ. The basal ganglia and motor control. Neural Plast 2003

Gur RE, Maany V, Mozley PD, Swanson C, Bilker W, Gur RC. Subcortical MRI volumes in neuroleptic-naive and treated patients with schizophrenia. Am J Psychiatry 1998; 155: 1711–1717.

Hafeman DM, Chang KD, Garrett AS, Sanders EM, Phillips ML. Effects of medication on neuroimaging findings in bipolar disorder: An updated review. Bipolar Disord 2012; 14: 375–410.

Hajek T, Kopecek M, Höschl C, Alda M. Smaller hippocampal volumes in patients with bipolar disorder are masked by exposure to lithium: A meta-analysis. J Psychiatry Neurosci 2012; 37: 333–343.

Halim ND, Weickert CS, McClintock BW, Weinberger DR, Lipska BK. Effects of chronic haloperidol and clozapine treatment on neurogenesis in the adult rat hippocampus. Neuropsychopharmacology 2004; 29: 1063–1069.

Hallahan B, Newell J, Soares JC, Brambilla P, Strakowski SM, Fleck DE, et al. Structural magnetic resonance imaging in bipolar disorder: An international collaborative mega-analysis of individual adult patient data. Biol Psychiatry 2011; 69: 326–335.

Hammonds MD, Shim SS. Effects of 4-week treatment with lithium and olanzapine on levels of brain-derived neurotrophic factor, B-Cell CLL/Lymphoma 2 and phosphorylated cyclic adenosine monophosphate response element-binding protein in the sub-regions of the hippocampus. Basic Clin Pharmacol Toxicol 2009; 105: 113–119.

Hashimoto R, Senatorov V, Kanai H, Leeds P, Chuang DM. Lithium stimulates progenitor proliferation in cultured brain neurons. Neuroscience 2003; 117: 55–61.

Herrero MT, Barcia C, Navarro JM. Functional anatomy of thalamus and basal ganglia. Child's Nerv Syst 2002; 18: 386–404.

Hibar DP, Westlye LT, Doan NT, Jahanshad N, Cheung JW, Ching CRK, et al. Cortical abnormalities in bipolar disorder: An MRI analysis of 6503 individuals from the ENIGMA Bipolar Disorder Working Group. Mol Psychiatry 2018; 23: 932–942.

Hibar DP, Westlye LT, Van Erp TGM, Rasmussen J, Leonardo CD, Faskowitz J, et al. Subcortical volumetric abnormalities in bipolar disorder. Mol Psychiatry 2016; 21: 1710–1716.

Hillary FG, Rajtmajer SM, Roman CA, Medaglia JD, Slocomb-Dluzen JE, Calhoun VD, et al. The rich get richer: Brain injury elicits hyperconnectivity in core subnetworks. PLoS One 2014; 9

Hillary FG, Roman CA, Venkatesan U, Rajtmajer SM, Bajo R, Castellanos ND. Hyperconnectivity is a fundamental response to neurological disruption. Neuropsychology 2015; 29: 59–75.

Iturria-Medina Y, Sotero RC, Toussaint PJ, Evans AC. Epidemic Spreading Model to Characterize Misfolded Proteins Propagation in Aging and Associated Neurodegenerative Disorders. PLoS Comput Biol 2014; 10

Janson AM, Fuxe K, Goldstein M, Deutch AY. Hypertrophy of dopamine neurons in the primate following ventromedial mesencephalic tegmentum lesion. Exp Brain Res 1991; 87: 232–238.

Jovicich J, Peters RJ, Koch C, Braun J, Chang L, Ernst T. Brain areas specific for attentional load in a motion-tracking task. J Cogn Neurosci 2001

Kempton MJ, Geddes JR, Ettinger U, Williams SCR, Grasby PM. Meta-analysis, database, and meta-regression of 98 structural imaging studies in bipolar disorder. Arch Gen Psychiatry 2008; 65: 1017–1032.

Kertzman C, Schwarz U, Zeffiro TA, Hallett M. The role of posterior parietal cortex in visually guided reaching movements in humans. Exp Brain Res 1997

Keshavan MS, Anderson S, Pettergrew JW. Is Schizophrenia due to excessive synaptic pruning in the prefrontal cortex? The Feinberg hypothesis revisited. J Psychiatr Res 1994; 28: 239–265.

Keshavan MS, Bagwell WW, Haas GL, Sweeney JA, Schooler NR, Pettegrew JW. Changes in caudate volume with neuroleptic treatment. Lancet 1994; 344: 1434.

Kippin TE, Kapur S, Van Der Kooy D. Dopamine specifically inhibits forebrain neural stem cell proliferation, suggesting a novel effect of antipsychotic drugs. J Neurosci 2005; 25: 5815–5823.

Kong J, White NS, Kwong KK, Vangel MG, Rosman IS, Gracely RH, et al. Using fMRI to dissociate sensory encoding from cognitive evaluation of heat pain intensity. Hum Brain Mapp 2006

Kreczmanski P, Heinsen H, Mantua V, Woltersdorf F, Masson T, Ulfig N, et al. Volume, neuron density and total neuron number in five subcortical regions in schizophrenia. Brain 2007; 130: 678–692.

Laird AR, Lancaster JL, Fox PT. BrainMap: The Social Evolution of a Human Brain Mapping Database. Neuroinformatics 2005; 3: 065–078.

Lang DJ, Kopala LC, Vandorpe RA, Rui Q, Smith GN, Goghari VM, et al. An MRI study of basal ganglia volumes in first-episode schizophrenia patients treated with risperidone. Am J Psychiatry 2001; 158: 625–631.

Lang DJ, Kopala LC, Vandorpe RA, Rui Q, Smith GN, Goghari VM, et al. Reduced basal ganglia volumes after switching to olanzapine in chronically treated patients with schizophrenia. Am J Psychiatry 2004; 161: 1829–1836.

Langner R, Sternkopf MA, Kellermann TS, Grefkes C, Kurth F, Schneider F, et al. Translating working memory into action: Behavioral and neural evidence for using motor representations in encoding visuo-spatial sequences. Hum Brain Mapp 2014; 35: 3465–3484.

Li L, Wu M, Liao Y, Ouyang L, Du M, Lei D, et al. Grey matter reduction associated with posttraumatic stress disorder and traumatic stress. Neurosci Biobehav Rev 2014; 43: 163–172.

Li Q, Zhao Y, Chen Z, Long J, Dai J, Huang X, et al. Meta-analysis of cortical thickness abnormalities in medication-free patients with major depressive disorder [Internet]. Neuropsychopharmacology 2019Available from: http://dx.doi.org/10.1038/s41386-019-0563-9

Li Y, Li W xiu, Xie D jie, Wang Y, Cheung EFC, Chan RCK. Grey matter reduction in the caudate nucleus in patients with persistent negative symptoms: An ALE meta-analysis. Schizophr Res 2018; 192: 9–15.

Liberati A, Altman DG, Tetzlaff J, Mulrow C, Gotzsche PC, Ioannidis JPA, et al. The PRISMA statement for reporting systematic reviews and meta-analyses of studies that evaluate healthcare interventions: explanation and elaboration. BMJ 2009; 339: b2700–b2700.

Lin C, Lee SH, Weng HH. Gray Matter Atrophy within the Default Mode Network of Fibromyalgia: A Meta-Analysis of Voxel-Based Morphometry Studies. Biomed Res Int 2016; 2016

Linkersdörfer J, Lonnemann J, Lindberg S, Hasselhorn M, Fiebach CJ. Grey matter alterations co-localize with functional abnormalities in developmental dyslexia: An ALE meta-analysis. PLoS One 2012; 7

López-Jaramillo C, Vargas C, Díaz-Zuluaga AM, Palacio JD, Castrillón G, Bearden C, et al. Increased hippocampal, thalamus and amygdala volume in long-term lithium-treated bipolar I disorder patients compared with unmedicated patients and healthy subjects. Bipolar Disord 2017; 19: 41–49.

Lord LD, Allen P, Expert P, Howes O, Broome M, Lambiotte R, et al. Functional brain networks before the onset of psychosis: A prospective fMRI study with graph theoretical analysis. NeuroImage Clin 2012; 1: 91–98.

Lotze M, Heymans U, Birbaumer N, Veit R, Erb M, Flor H, et al. Differential cerebral activation during observation of expressive gestures and motor acts. Neuropsychologia 2006; 44: 1787–1795.

Lu CL, Wu YT, Yeh TC, Chen LF, Chang FY, Lee SD, et al. Neuronal correlates of gastric pain induced by fundus distension: A 3T-fMRI study. Neurogastroenterol Motil 2004

Lu X, Zhong Y, Ma Z, Wu Y, Fox PT, Zhang N, et al. Structural imaging biomarkers for bipolar disorder: Meta-analyses of whole-brain voxel-based morphometry studies. Depress Anxiety 2019; 36: 353–364.

Lyoo IK, Dager SR, Kim JE, Yoon SJ, Friedman SD, Dunner DL, et al. Lithium-induced gray matter volume increase as a neural correlate of treatment response in bipolar disorder: A longitudinal brain imaging study. Neuropsychopharmacology 2010; 35: 1743–1750.

Mancuso L, Costa T, Nani A, Manuello J, Liloia D, Gelmini G, et al. The homotopic connectivity of the functional brain: a meta-analytic approach. Sci Rep 2019; 9: 3346.

Manji HK, Moore GJ, Chen G. Lithium up-regulates the cytoprotective protein Bcl-2 in the CNS in vivo: A role for neurotrophic and neuroprotective effects in manic depressive illness. J Clin Psychiatry 1997

Manji HK, Moore GJ, Chen G. Lithium at 50: Have the neuroprotective effects of this unique cation been overlooked? Biol Psychiatry 1999; 46: 929–940.

Manuello J, Nani A, Premi E, Borroni B, Costa T, Tatu K, et al. The pathoconnectivity profile of Alzheimer's disease: A morphometric coalteration network analysis. Front Neurol 2018; 8: 1–15.

Maslov S, Sneppen K. Specificity and Stability in Topology of Protein Networks. Science (80-) 2002; 296: 910–913.

Massana G, Salgado-Pineda P, Junqué C, Pérez M, Baeza I, Pons A, et al. Volume changes in gray matter in first-episode neuroleptic-naive schizophrenic patients treated with risperidone. J Clin Psychopharmacol 2005; 25: 111–117.

McTeague LM, Goodkind MS, Etkin A. Transdiagnostic impairment of cognitive control in mental illness. J Psychiatr Res 2016; 83: 37–46.

McTeague LM, Huemer J, Carreon DM, Jiang Y, Eickhoff SB, Etkin A. Identification of common neural circuit disruptions in cognitive control across psychiatric disorders. Am J Psychiatry 2017; 174: 676–685.

Moher D, Liberati A, Tetzlaff J, Altman DG. Preferred Reporting Items for Systematic Reviews and Meta-Analyses: The PRISMA Statement. J Clin Epidemiol 2009; 62: 1006–1012.

Monkul ES, Matsuo K, Nicoletti MA, Dierschke N, Hatch JP, Dalwani M, et al. Prefrontal gray matter increases in healthy individuals after lithium treatment: A voxel-based morphometry study. Neurosci Lett 2007; 429: 7–11.

Moore GJ, Bebchuk JM, Wilds IB, Chen G, Menji HK. Lithium-induced increase in human brain grey matter. Lancet 2000; 356: 1241–1242.

Muller P, Seeman P. Brain neurotransmitter receptors after long-term haloperidol: Dopamine, acetylcholine, serotonin, α-noradrenergic and naloxone receptors. Life Sci 1977; 21: 1751–1758.

Murali P, Doraiswamy, Tupler L, Ranga Rama Krishnan K. Neuroleptic treatment and caudate plasticity. Lancet 1995; 345: 734–735.

Nagy A, Eördegh G, Paróczy Z, Márkus Z, Benedek G. Multisensory integration in the basal ganglia. Eur J Neurosci 2006

Naito E, Scheperjans F, Eickhoff SB, Amunts K, Roland PE, Zilles K, et al. Human superior parietal lobule is involved in somatic perception of bimanual interaction with an external object. J Neurophysiol 2008

Navari S, Dazzan P. Do antipsychotic drugs affect brain structure? A systematic and critical review of MRI findings. Psychol Med 2009; 39: 1763–1777.

Oertel-Knöchel V, Knöchel C, Matura S, Rotarska-Jagiela A, Magerkurth J, Prvulovic D, et al. Cortical-basal ganglia imbalance in schizophrenia patients and unaffected first-degree relatives. Schizophr Res 2012; 138: 120–127.

Olausson H, Charron J, Marchand S, Villemure C, Strigo IA, Bushnell MC. Feelings of warmth correlate with neural activity in right anterior insular cortex. Neurosci Lett 2005

Olausson H, Lamarre Y, Backlund H, Morin C, Wallin BG, Starck G, et al. Unmyelinated tactile afferents signal touch and project to insular cortex. Nat Neurosci 2002

Palaniyappan L. Inefficient neural system stabilization: a theory of spontaneous resolutions and recurrent relapses in psychosis. J Psychiatry Neurosci 2019; 44: 1–17.

Palaniyappan L, Liddle PF. Does the salience network play a cardinal role in psychosis? An emerging hypothesis of insular dysfunction. J Psychiatry Neurosci 2012; 37: 17–27.

Park SW, Lee SK, Kim JM, Yoon JS, Kim YH. Effects of quetiapine on the brain-derived neurotrophic factor expression in the hippocampus and neocortex of rats. Neurosci Lett 2006; 402: 25–29.

Patel RS, Bowman FD, Rilling JK. A Bayesian approach to determining connectivity of the human brain. Hum Brain Mapp 2006; 27: 267–276.

Poletti S, Leone G, Hoogenboezem TA, Ghiglino D, Vai B, de Wit H, et al. Markers of neuroinflammation influence measures of cortical thickness in bipolar depression. Psychiatry Res - Neuroimaging 2019; 285: 64–66.

Power JD, Barnes K, Snyder A. Spurious but systematic correlations in resting state functional connectivity MRI arise from head motion. Neuroimage 2012; 59: 2142–2154.

Qiu L, Lui S, Kuang W, Huang X, Li J, Li J, et al. Regional increases of cortical thickness in untreated, first-episode major depressive disorder. Transl Psychiatry 2014; 4

Raj A, Kuceyeski A, Weiner M. A Network Diffusion Model of Disease Progression in Dementia. Neuron 2012; 73: 1204–1215.

Raj A, Powell F. Models of Network Spread and Network Degeneration in Brain Disorders. Biol Psychiatry Cogn Neurosci Neuroimaging 2018; 3: 788–797.

Reynolds S, Carrey N, Jaworska N, Langevin LM, Yang XR, MacMaster FP. Cortical thickness in youth with major depressive disorder. BMC Psychiatry 2014; 14

Robbe D. To move or to sense? Incorporating somatosensory representation into striatal functions. Curr Opin Neurobiol 2018

Rocha E, Achaval M, Santos P, Rodnight R. Lithium treatment causes gliosis and modifies the morphology of hippocampal astrocytes in rats. Neuroreport 1998; 9: 3971–3974.

Rubinov M, Sporns O. Complex network measures of brain connectivity: Uses and interpretations. Neuroimage 2010; 52: 1059–1069.

Sarrazin S, Poupon C, Teillac A, Mangin JF, Polosan M, Favre P, et al. Higher in vivo cortical intracellular volume fraction associated with lithium therapy in bipolar disorder: A multicenter noddi study. Psychother Psychosom 2019; 88: 171–176.

Sassi RB, Nicoletti M, Brambilla P, Mallinger AG, Frank E, Kupfer DJ, et al. Increased gray matter volume in lithium-treated bipolar disorder patients. Neurosci Lett 2002; 329: 243–245.

Scarpazza C, Tognin S, Frisciata S, Sartori G, Mechelli A. False positive rates in Voxel-based Morphometry studies of the human brain: Should we be worried? Neurosci Biobehav Rev 2015; 52: 49–55.

Scheepers FE, De Wied CCG, Pol HEH, Van De Flier W, Van Der Linden JA, Kahn RS. The effect of clozapine on caudate nucleus volume in schizophrenic patients previously treated with typical antipsychotics. Neuropsychopharmacology 2001; 24: 47–54.

Schoedel ALA, Zimmermann K, Handwerker HO, Forster C. The influence of simultaneous ratings on cortical BOLD effects during painful and non-painful stimulation. Pain 2008

Sedvall G, Pauli S, Farde L, Karlsson P, Nyberg S, Nordström AL. Recent developments in PET scan imaging of neuroreceptors in schizophrenia. Isr J Psychiatry Relat Sci 1995

Seeley WW, Crawford RK, Zhou J, Miller BL, Greicius MD. Neurodegenerative Diseases Target Large-Scale Human Brain Networks. Neuron 2009; 62: 42–52.

Sesack SR, Carr DB. Selective prefrontal cortex inputs to dopamine cells: Implications for schizophrenia. Physiol Behav 2002; 77: 513–517.

Sha Z, Wager TD, Mechelli A, He Y. Common Dysfunction of Large-Scale Neurocognitive Networks Across Psychiatric Disorders. Biol Psychiatry 2019; 85: 379–388.

Shafiei G, Markello RD, Makowski C, Talpalaru A, Kirschner M, Devenyi GA, et al. Spatial patterning of tissue volume loss in schizophrenia reflects brain network architecture. Biol Psychiatry 2019: 626168.

Sheffield JM, Kandala S, Tamminga CA, Pearlson GD, Keshavan MS, Sweeney JA, et al. Transdiagnostic associations between functional brain network integrity and cognition. JAMA Psychiatry 2017; 74: 605–613.

Sheline YI, Gado MH, Kraemer HC. Untreated Depression and Hippocampal Volume Loss. Am J Psychiatry 2003; 160: 1516–1518.

Shihabuddin L, Buchsbaum MS, Hazlett EA, Haznedar MM, Harvey PD, Newman A, et al. Dorsal striatal size, shape, and metabolic rate in never-medicated and previously medicated schizophrenics performing a verbal learning task. Arch Gen Psychiatry 1998; 55: 235–243.

Smith SM, Miller KL, Salimi-Khorshidi G, Webster M, Beckmann CF, Nichols TE, et al. Network modelling methods for FMRI. Neuroimage 2011; 54: 875–891.

Stephan KM, Fink GR, Passingham RE, Silbersweig D, Ceballos-Baumann AO, Frith CD, et al. Functional anatomy of the mental representation of upper extremity movements in healthy subjects. J Neurophysiol 1995

Stevens JR. Abnormal reinnervation as a basis for schizophrenia: A hypothesis. Arch Gen Psychiatry 1992: 10–15.

Stoeckel MC, Weder B, Binkofski F, Choi HJ, Amunts K, Pieperhoff P, et al. Left and right superior parietal lobule in tactile object discrimination. Eur J Neurosci 2004

Stoodley CJ. Distinct regions of the cerebellum show gray matter decreases in autism, ADHD, and developmental dyslexia. Front Syst Neurosci 2014; 8: 1–17.

Strigo IA, Duncan GH, Boivin M, Bushnell MC. Differentiation of visceral and cutaneous pain in the human brain. J Neurophysiol 2003

Strungas S, Christensen JD, Holcomb JM, Garver DL. State-related thalamic changes during antipsychotic treatment in schizophrenia: Preliminary observations. Psychiatry Res - Neuroimaging 2003; 124: 121–124.

Suh JS, Schneider MA, Minuzzi L, MacQueen GM, Strother SC, Kennedy SH, et al. Cortical thickness in major depressive disorder: A systematic review and meta-analysis. Prog Neuro-Psychopharmacology Biol Psychiatry 2019; 88: 287–302.

Tan H-Y, Sust S, Buckholtz JW, Mattay VS, Meyer-Lindenberg A, Egan MF, et al. Dysfunctional Prefrontal Regional Specialization and Compensation in Schizophrenia. Am J Psychiatry 2006; 163: 1969–1977.

Tatu K, Costa T, Nani A, Diano M, Quarta DG, Duca S, et al. How do morphological alterations caused by chronic pain distribute across the brain? A meta-analytic co-alteration study. NeuroImage Clin 2018; 18: 15–30.

Torres US, Portela-Oliveira E, Borgwardt S, Busatto GF. Structural brain changes associated with antipsychotic treatment in schizophrenia as revealed by voxel-based morphometric MRI: An activation likelihood estimation meta-analysis. BMC Psychiatry 2013; 13

Tseng MT, Tseng WYI, Chao CC, Lin HE, Hsieh ST. Distinct and shared cerebral activations in processing innocuous versus noxious contact heat revealed by functional magnetic resonance imaging. Hum Brain Mapp 2010

Turkeltaub PE, Eickhoff SB, Laird AR, Fox M, Wiener M, Fox P. Minimizing within-experiment and within-group effects in activation likelihood estimation meta-analyses. Hum Brain Mapp 2012; 33: 1–13.

Vanasse TJ, Fox PM, Barron DS, Robertson M, Eickhoff SB, Lancaster JL, et al. BrainMap VBM: An environment for structural meta-analysis. Hum Brain Mapp 2018; 39: 3308–3325.

Wada A, Yokoo H, Yanagita T, Kobayashi H. Lithium: Potential therapeutics against acute brain injuries and chronic neurodegenerative diseases. J Pharmacol Sci 2005; 99: 307–321.

Wakade CG, Mahadik SP, Waller JL, Chiu FC. Atypical neuroleptics stimulate neurogenesis in adult rat brain. J Neurosci Res 2002; 69: 72–79.

Wang HD, Dunnavant FD, Jarman T, Deutch AY. Effects of antipsychotic drugs on neurogenesis in the forebrain of the adult rat. Neuropsychopharmacology 2004; 29: 1230–1238.

Wang Y, David O, Hu X, Deshpande G. Can Patel's τ accurately estimate directionality of connections in brain networks from fMRI? Magn Reson Med 2017; 78: 2003–2010.

Weinberger DR, Radulescu E. Finding the elusive psychiatric 'lesion' with 21st-century neuroanatomy: A note of caution. Am J Psychiatry 2016; 173: 27–33.

Westmoreland Corson P, Nopoulos P, Miller DD, Arndt S, Andreasen NC. Change in basal ganglia volume over 2 years in patients with schizophrenia: Typical versus atypical neuroleptics. Am J Psychiatry 1999; 156: 1200–1204.

Wise T, Radua J, Via E, Cardoner N, Abe O, Adams TM, et al. Common and distinct patterns of grey-matter volume alteration in major depression and bipolar disorder: Evidence from voxel-based meta-analysis. Mol Psychiatry 2017; 22: 1455–1463.

World Health Organisation. The ICD-10 classification of mental and behavioural disorders: clinical descriptions and diagnostic guidelines. World Heal Organ 1992

Wu Y, Zhong Y, Ma Z, Lu X, Zhang N, Fox PT, et al. Gray matter changes in panic disorder: A voxel-based meta-analysis and meta-analytic connectivity modeling. Psychiatry Res - Neuroimaging 2018; 282: 82–89.

Yan CG, Wang X Di, Zuo XN, Zang YF. DPABI: Data Processing & Analysis for (Resting-State) Brain Imaging. Neuroinformatics 2016; 14: 339–351.

Yang X hua, Wang Y, Huang J, Zhu C ying, Liu X qun, Cheung EFC, et al. Increased prefrontal and parietal cortical thickness does not correlate with anhedonia in patients with untreated first-episode major depressive disorders. Psychiatry Res - Neuroimaging 2015; 234: 144–151.

Yates D. Neurodegenerative disease: Neurodegenerative networking. Nat Rev Neurosci 2012; 13: 288–

289.

Yau Y, Zeighami Y, Baker TE, Larcher K, Vainik U, Dadar M, et al. Network connectivity determines cortical thinning in early Parkinson's disease progression. Nat Commun 2018; 9: 12.

Yeo BTT, Krienen FM, Sepulcre J, Sabuncu MR, Lashkari D, Hollinshead M, et al. The organization of the human cerebral cortex estimated by intrinsic functional connectivity. J Neurophysiol 2011; 106: 1125–1165.

Yoo SS, Freeman DK, McCarthyIII JJ, Jolesz FA. Neural substrates of tactile imagery: A functional MRI study. Neuroreport 2003

Yucel K, McKinnon MC, Taylor VH, Macdonald K, Alda M, Young LT, et al. Bilateral hippocampal volume increases after long-term lithium treatment in patients with bipolar disorder: A longitudinal MRI study. Psychopharmacology (Berl) 2007; 195: 357–367.

Yucel K, Taylor VH, McKinnon MC, MacDonald K, Alda M, Young LT, et al. Bilateral hippocampal volume increase in patients with bipolar disorder and short-term lithium treatment. Neuropsychopharmacology 2008; 33: 361–367.

Zalesky A, Fornito A, Harding IH, Cocchi L, Yücel M, Pantelis C, et al. Whole-brain anatomical networks: Does the choice of nodes matter? Neuroimage 2010; 50: 970–983.

Zatorre RJ, Fields RD, Johansen-Berg H. Plasticity in gray and white: neuroimaging changes in brain structure during learning. Nat Neurosci 2012; 15: 528–536.

Zeighami Y, Ulla M, Iturria-Medina Y, Dadar M, Zhang Y, Larcher KMH, et al. Network structure of brain atrophy in de novo parkinson's disease. Elife 2015; 4: 1–20.

Zheng Y-Q, Zhang Y, Yau Y, Zeighami Y, Larcher K, Misic B, et al. Local vulnerability and global connectivity jointly shape neurodegenerative disease propagation. PLOS Biol 2019; 17: 1–27.

Zhou J, Gennatas ED, Kramer JH, Miller BL, Seeley WW. Predicting Regional Neurodegeneration from the Healthy Brain Functional Connectome. Neuron 2012; 73: 1216–1227.

Zung S, Souza-Duran FL, Soeiro-De-souza MG, Uchida R, Bottino CM, Busatto GF, et al. The influence of lithium on hippocampal volume in elderly bipolar patients: A study using voxel-based morphometry. Transl Psychiatry 2016; 6: 1–7.

Zuo Z, Ran S, Wang Y, Li C, Han Q, Tang Q, et al. Altered structural covariance among the dorsolateral prefrontal cortex and amygdala in treatment-Naïve patients with major depressive disorder. Front

Psychiatry 2018; 9: 1–10.

Table 1: summary of the pathologies obtained by the first selection of studies. Experiments about psychiatric disorders were included in the meta-analysis, while those about neurological disorders were excluded.

included	**Diagnosis**	**ICD-10 code**	Number of experiments for condition
yes	Schizophrenia	F20	25
yes	Pervasive developmental disorders, autism	F84	13
yes	Bipolar disorder	F31	7
yes	Major depressive disorder	F31-33	7
yes	Obsessive-compulsive disorder	F42	6
yes	Attention deficit/hyperactivity disorder	F90	2
yes	Specific developmental disorders of speech and language	F80	2
yes	Other disorders of psychological development, Tourette syndrome	F95	1
yes	Other psychotic disorder not due to a substance or known physiological condition	F28	1
no	Epilepsy and Recurrent Seizures TLE, JME	G40	13

no	Other extrapyramidal and movement disorders	G25	4
no	Dystonia	G24	2
no	Parkinson's Disease PD, ET	G20	2

Table 2: list of experiments obtained by the first selection of studies.. Each entry of the list represents an experiment of decrease and one of increase. Experiments about psychiatric disorders were included in the meta-analysis, while those about neurological disorders were excluded.

included	**author**	**# subjects**	**ICD-10 code**	**Diagnosis**
yes	Abell F, 1999	15	F84	Pervasive Developmental Disorders PDD, autism, ASD
yes	Adler CM, 2005	27	F31	Bipolar Disorder BD, BPD
yes	Antonova E, 2005	40	F20	Schizophrenia SZ
yes	Arnone D, 2009	25	F32-F33	Major Depressive Disorder
yes	Arnone D, 2013	39	F32-F33	Major Depressive Disorder
yes	Bassitt DP, 2007	30	F20	Schizophrenia SZ
yes	Brieber S, 2007	15	F84	Pervasive Developmental Disorders PDD, autism, ASD
yes	Brieber S, 2007	15	F90	Attention Deficit/Hyperactivity Disorder
yes	Cheng Y, 2011	25	F84	Pervasive Developmental Disorders PDD, autism, ASD
yes	Cheng Y, 2011	11	F84	Pervasive Developmental Disorders PDD, autism, ASD
yes	Cheng Y, 2011	12	F84	Pervasive Developmental Disorders PDD, autism, ASD
yes	Cheng Y, 2011	12	F84	Pervasive Developmental Disorders PDD, autism, ASD
yes	Cui L, 2011	23	F20	Schizophrenia SZ
yes	Cui L, 2011	24	F31	Bipolar Disorder BD, BPD
yes	Deng MY, 2009	10	F20	Schizophrenia SZ
yes	Deng MY, 2009	10	F20	Schizophrenia SZ

yes	Ecker C, 2010	22	F84	Pervasive Developmental Disorders PDD, autism, ASD
yes	Ecker C, 2012	89	F84	Pervasive Developmental Disorders PDD, autism, ASD
yes	Gilbert AR, 2008	20	F42	Obsessive Compulsive Disorder OCD
yes	Giuliani NR, 2005	34	F20	Schizophrenia SZ
yes	Gong Q, 2011	23	F32-F33	Major Depressive Disorder
yes	Gong Q, 2011	23	F32-F33	Major Depressive Disorder
yes	Haldane M, 2008	44	F31	Bipolar Disorder BD, BPD
yes	Ha TH, 2004	35	F20	Schizophrenia SZ
yes	Honea RA, 2008	169	F20	Schizophrenia SZ
yes	Hulshoff Pol HE, 2001	158	F20	Schizophrenia SZ
yes	Hwang J, 2010	26	F32-F33	Major Depressive Disorder
yes	Hyde KL, 2010	13	F84	Pervasive Developmental Disorders PDD, autism, ASD
yes	Kasparek T, 2010	49	F20	Schizophrenia SZ
yes	Kawasaki Y, 2004	25	F20	Schizophrenia SZ
yes	Ke X, 2008	15	F84	Pervasive Developmental Disorders PDD, autism, ASD
yes	Ladoucer CD, 2008	20	F31	Bipolar Disorder BD, BPD
yes	Leung KK, 2009	17	F32-F33	Major Depressive Disorder
yes	Lu C, 2010	12	F80	Specific Developmental Disorders of Speech and Language
yes	Ludolph AG, 2006	14	F95	Other Disorders of Psychological Development. Tourette
yes	Marcelis M, 2003	27	F28	Other psychotic disorder not due to a substance or known physiological condition
yes	Mengotti P, 2011	20	F84	Pervasive Developmental Disorders PDD, autism, ASD
yes	Molina V, 2011	24	F20	Schizophrenia SZ
yes	Molina V, 2011	30	F20	Schizophrenia SZ
yes	O'Daly O, 2007	28	F20	Schizophrenia SZ
yes	Price G, 2010	47	F20	Schizophrenia SZ
yes	Pujol J, 2004	72	F42	Obsessive Compulsive Disorder OCD
yes	Salgado-Pineda P, 2003	13	F20	Schizophrenia SZ

yes	Salmond CH, 2007	9	F84	Pervasive Developmental Disorders PDD, autism, ASD
yes	Saricicek A, 2015	28	F31	Bipolar Disorder BD, BPD
yes	Scheuerecker J, 2010	13	F32-F33	Major Depressive Disorder
yes	Schiffer B, 2013	25	F20	Schizophrenia SZ
yes	Shapleske J, 2002	31	F20	Schizophrenia SZ
yes	Shapleske J, 2002	32	F20	Schizophrenia SZ
yes	SmesnyS,2010	13	F20	Schizophrenia SZ
yes	Smesny S, 2010	11	F20	Schizophrenia SZ
yes	Suzuki M, 2002	42	F20	Schizophrenia SZ
yes	Szeszko PR, 2008	26	F42	Obsessive Compulsive Disorder OCD
yes	Tang LR, 2014	27	F31	Bipolar Disorder BD, BPD
yes	Toal F, 2010	26	F84	Pervasive Developmental Disorders PDD, autism, ASD
yes	Valente AA Jr, 2005	15	F42	Obsessive Compulsive Disorder OCD
yes	Valente AA Jr, 2005	15	F42	Obsessive Compulsive Disorder OCD
yes	Wang J, 2007	12	F90	Attention Deficit/Hyperactivity Disorder
yes	Watkins KE, 2002	10	F80	Specific Developmental Disorders of Speech and Language
yes	Watson DR, 2012	25	F20	Schizophrenia SZ
yes	Watson DR, 2012	24	F31	Bipolar Disorder BD, BPD
yes	Whitford TJ, 2006	41	F20	Schizophrenia SZ
yes	Wilke M, 2001	48	F20	Schizophrenia SZ
yes	Yoo SY, 2008	47	F42	Obsessive Compulsive Disorder OCD
no	Celle S, 2010	17	G25	Other extrapyramidal and movement disorders
no	Chan CH, 2006	13	G40	Epilepsy and Recurrent Seizures TLE, JME
no	De Araujo-Filho GM,	16	G40	Epilepsy and Recurrent Seizures TLE, JME

	2009			
no	Etgen T, 2005	28	G25	Other extrapyramidal and movement disorders
no	Granert O, 2011	11	G24	Dystonia
no	Keller SS, 2002	40	G40	Epilepsy and Recurrent Seizures TLE, JME
no	Keller SS, 2002	36	G40	Epilepsy and Recurrent Seizures TLE, JME
no	Keller SS, 2002	58	G40	Epilepsy and Recurrent Seizures TLE, JME
no	Keller SS, 2002	58	G40	Epilepsy and Recurrent Seizures TLE, JME
no	Keller SS, 2002	58	G40	Epilepsy and Recurrent Seizures TLE, JME
no	Kim JH, 2007	25	G40	Epilepsy and Recurrent Seizures TLE, JME
no	Lin CH, 2013	10	G20	Parkinson's Disease PD, ET
no	Lin CH, 2013	10	G20	Parkinson's Disease PD, ET
no	Lin CH, 2013	10	G25	Other extrapyramidal and movement disorders
no	Lin CH, 2013	10	G25	Other extrapyramidal and movement disorders
no	Lin K, 2009	30	G40	Epilepsy and Recurrent Seizures TLE, JME
no	Lin K, 2009	19	G40	Epilepsy and Recurrent Seizures TLE, JME
no	Lin K, 2009	30	G40	Epilepsy and Recurrent Seizures TLE, JME
no	Obermann M, 2007	9	G24	Dystonia
no	Riederer F, 2008	12	G40	Epilepsy and Recurrent Seizures TLE, JME
no	Riederer F, 2008	12	G40	Epilepsy and Recurrent Seizures TLE, JME

Table 2: list of experiments of increase included and excluded in the main analysis

Table 3: alteration states and marginal probability.

Node a	Node b			
		Altered	Non-altered	
	Altered	ϑ_1	ϑ_3	$\vartheta_1 + \vartheta_3$
	Non-altered	ϑ_2	ϑ_4	$\vartheta_2 + \vartheta_4$

		$\vartheta_1 + \vartheta_2$	$\vartheta_3 + \vartheta_4$	1

Table 4: the 25 nodes with the highest strength

Node	x	y	z	Type of alteration	Strength
Left BA 13	-42	16	0	decrease	8.33
Left Thalamus	-2	-18	6	decrease	7.74
Left BA 47	-40	26	-6	decrease	7.35
Left BA 35 (Parahippocampal gyrus)	-26	-20	-20	both decrease and increase	7.2
Left BA 47	-36	16	-8	decrease	6.89
Left Putamen	-22	0	12	increase	6.47
Left BA 28	-14	-16	-20	both decrease and increase	6.36
Left Amygdala	-18	-8	-14	both decrease and increase	6.27
Left BA 5	-4	-42	50	increase	5.94
Left Thalamus	-8	-22	-2	decrease	5.63
Left BA 36 (Parahippocampal gyrus)	-32	-12	-20	both decrease and increase	5.59
Left Putamen	-28	-8	12	increase	5.36
Left Thalamus	-10	-10	0	both decrease and increase	5.23
Left BA 13	-40	2	12	both decrease and increase	5.23
Right Putamen	22	2	2	both decrease and increase	5.18
Left Caudate Body	-10	10	12	both decrease and increase	5.17
Left BA 32	-16	34	24	decrease	5.03
Left Putamen	-22	8	6	increase	5.01
Left BA 9	-6	40	24	decrease	4.85
Right BA 40	40	-56	38	decrease	4.83
Left BA 32	-12	36	14	decrease	4.83

Left BA 47	-32	26	0	both decrease and increase	4.82
Right BA 5	10	-42	66	increase	4.57
Right BA 5	4	-44	56	increase	4.34
Left BA 47	-28	22	-10	both decrease and increase	4.29

Figure captions

Figure 1: illustration of the methods for the calculation of the decrease-increase association matrix. **A**: the untresholded ALE maps of the decreases and the increases databases are merged. **B**: such map is fed to a peak detection algorithm to obtain the nodes of the network; **C**: each node is considered altered in each experiment if the 20% of its voxels are covered by a significant MA map voxel of that experiment. This operation produce a vector of 1 and 0 for each node that describes if that node is altered or not in each experiment, creating two alteration matrices, one for the decreases, one for the increases. **D**: the Patel's κ is calculated between each node vector of the decreases alteration matrix and each node vector of the increases alteration matrix. This produces a matrix of co-alteration between the decreases and the increases, which gives us the intensity of the edges of the network.

Figure 2: **A**: network of co-alterations of opposite GM changes, showing the unconnected nodes in grey color. **B**: network of co-alterations of opposite GM changes. **C**: nodal strength of the network. The size of the nodes is proportional to the weighted degree centrality.

Figure 3: **A** and **B**: co-alteration networks represented in 2D, dividing each node for one of the Yeo7 RSN, plus cerebellum and thalamus/basal ganglia. The size of the nodes is proportional to the degree centrality, standardized across networks. DAN: dorsal attention network; DMN: default mode network; ECN: executive control network; Vis: visual network; S/VAN: salience/ventral attention network; Thal/BG: thalamus and basal ganglia, comprising upper midbrain. **A**: Decrease-increase co-alteration network. The transparency of the edge is inversely proportional to its κ value. Note that the arrows do not mean that the network is directed in a strict sense as the Patel's κ is not a measure that provide a directionality. However, each edge links two nodes of different modality: one is a decrease and the other is an increase. Arrows were used to indicate at which side of the edge is the increase node. **B**: decrease only and increase only co-alteration networks. **C**: plot of the 30 runs of the Fail-safe analysis. On the x-axis: level of the null model. For each level, 10 random modelled alteration maps were added to the database. On the y-axis: values of Pearson's r between the original decrease-increase association network and each of the level of the model. **D**: plot of the 30 runs of the dummy-pairs analysis with control decreases plus dummy increases. **E**: plot of the 30 runs of the dummy-pairs analysis with control increases plus dummy decreases.

Figure 4: **A**: directed network of decrease-increase co-alteration. Positive edges indicates that the decrease node is dominant on, and possibly influences, the increase node. Negative edges indicates the opposite. **B**: hubs of the directed network, divided for positive hubs (left) and negative hubs (right). Note that these images were produced calculating the strength of each node on the whole Patel's τ matrix, and then separated between the nodes with a positive value and those with a negative value. Thus, the strength of each node represents its balance between the positive and negative edges incident upon it. Therefore the size of the node is not proportional to the number of its edges, since positive and negative edges incident upon a same node cancel each other. See Supplementary Figure S5 for a representation of the strength of positive-only and and negative-only edges. **C**: 2D representation of the directed network. Positive edges indicates that the decrease node is dominant on, and possibly influences, the increase node. Negative edges indicates the opposite. DAN: dorsal attention network; DMN: default mode network; ECN: executive control network; Vis: visual network; S/VAN: salience/ventral attention network; Thal/BG: thalamus and basal ganglia, comprising upper midbrain.

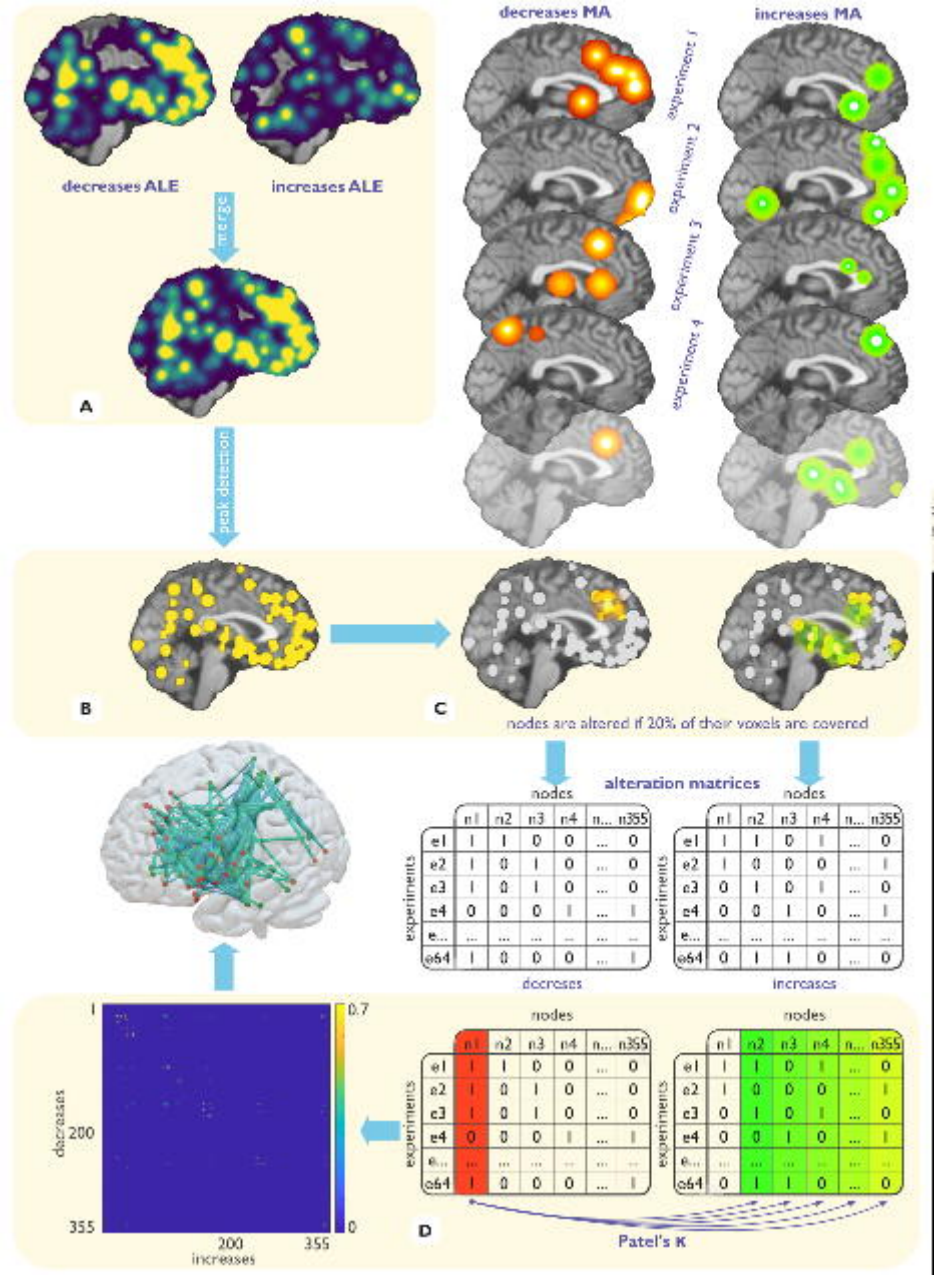
decreases ALE
increases ALE
merge
A
peak detection
decreases MA
increases MA
experiment 1
experiment 2
experiment 3
experiment 4
B
C
nodes are altered if 20% of their voxels are covered
alteration matrices
nodes
experiments
decreases
increases
D
Patel's K
decreases
increases
0.7
0
1
200
355

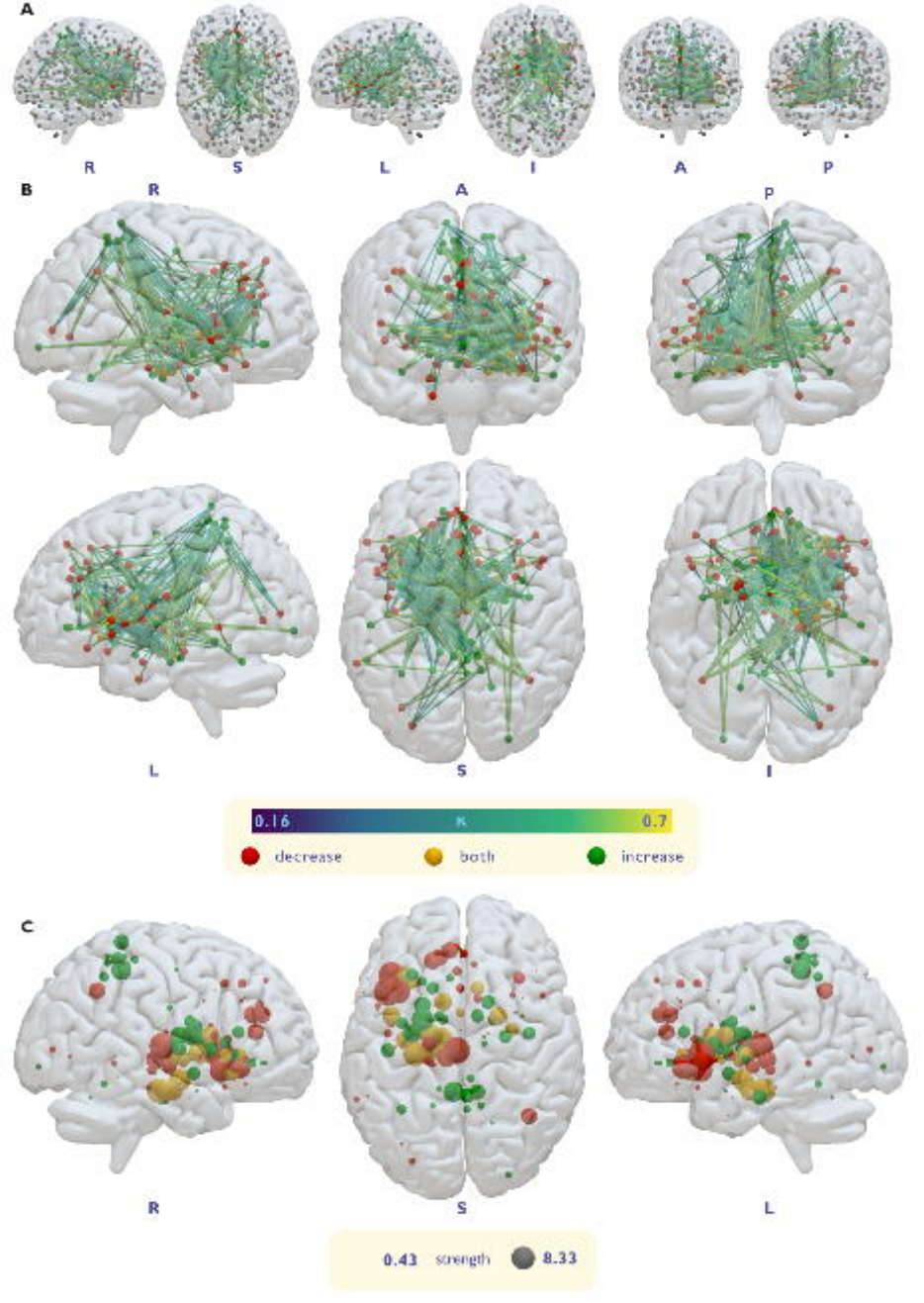
A
R
S
L
I
A
P
B
R
A
P
L
S
I
0.16
K
0.7
decrease
both
increase
C
R
S
L
0.43
strength
8.33

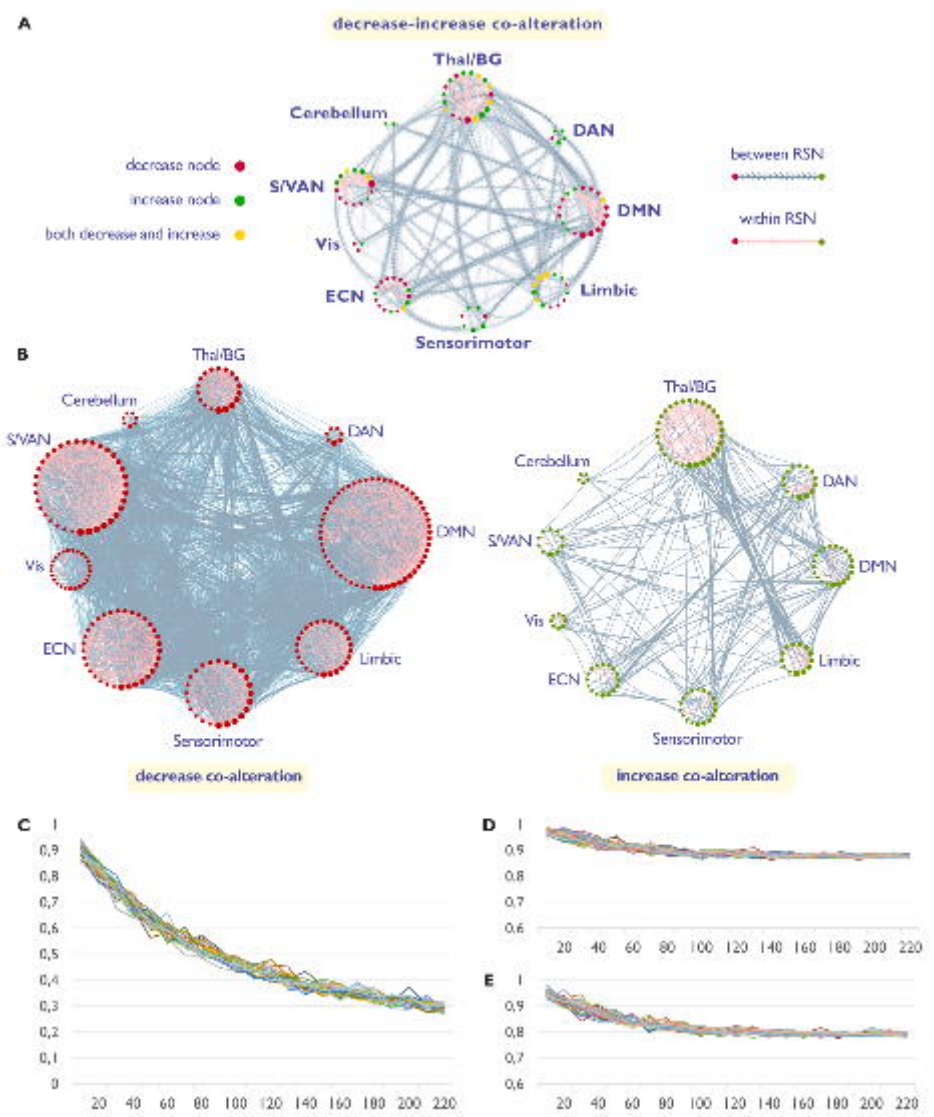
A
decrease-increase co-alteration
Thal/BG
Cerebellum
DAN
S/VAN
DMN
Vis
Limbic
ECN
Sensorimotor
decrease node
increase node
both decrease and increase
between RSN
within RSN
B
Thal/BG
Cerebellum
DAN
S/VAN
DMN
Vis
Limbic
ECN
Sensorimotor
decrease co-alteration
increase co-alteration
C
D
E
1
0,9
0,8
0,7
0,6
0,5
0,4
0,3
0,2
0,1
0
20 40 60 80 100 120 140 160 180 200 220

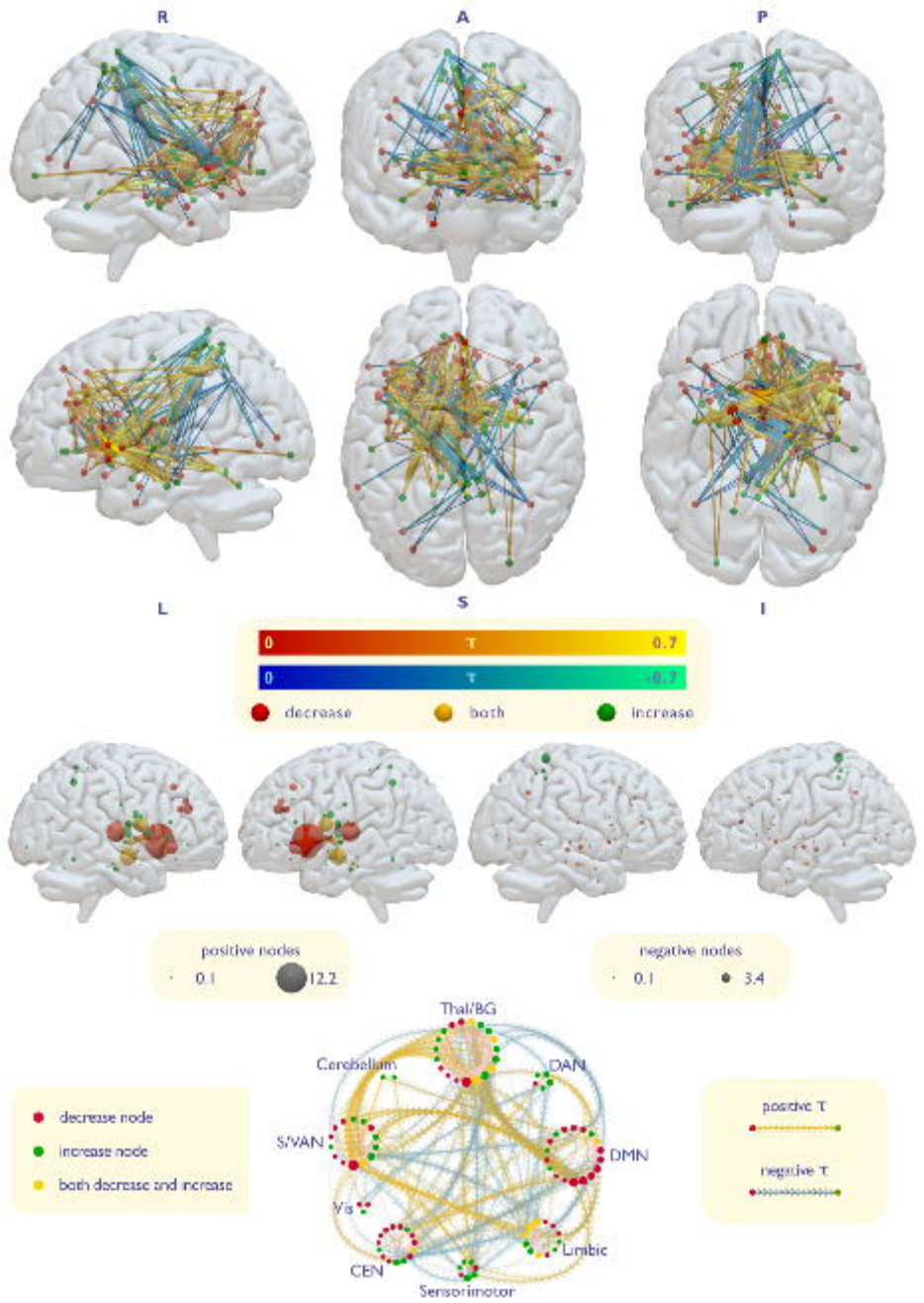
R
A
P
L
S
I
0
τ
0.7
0
τ
-0.7
decrease
both
increase
positive nodes
0.1
12.2
negative nodes
0.1
3.4
Thal/BG
Cerebellum
DAN
SVAN
DMN
Vis
Limbic
CEN
Sensorimotor
decrease node
increase node
both decrease and increase
positive τ
negative τ